Food and Bioprocess Technology
https://doi.org/10.1007/s11947-025-03959-7

RESEARCH

Active Bilayer Material Formed by Starch Film and Thyme Essential Oil Encapsulated into Zein Electrospun Fibers

Jéssica Silveira Vitoria[1] · Laura Martins Fonseca[2] · Tatiane Jéssica Siebeneichler[2] · Débora Campos[3] · Fátima Poças[3] · Maria Manuela Estevez Pintado[3] · Elessandra da Rosa Zavareze[2] · Eliezer Avila Gandra[1]

Received: 31 March 2025 / Accepted: 4 July 2025

Abstract

This study aimed to develop bilayer films based on sweet potato starch (4.0%, w/v) with zein electrospun fibers (30%, w/v) encapsulating thyme essential oil (TEO) (60%, v/w). It is hypothesized that the bilayer material exhibits enhanced physicochemical properties, improved thermal stability, reduced water vapor permeability, adequate mechanical strength, and controlled TEO release. This approach offers a sustainable food packaging alternative with bioactive potential in food preservation. The TEO was analyzed for its chemical composition, while the bilayer films and their components were assessed for morphology, FT-IR absorption profile, thermal properties, color, moisture content, solubility, water vapor permeability, thickness, mechanical properties, contact angle, biodegradability, loading capacity, encapsulation efficiency, TEO release, and antioxidant activity. *p*-cymene was identified as the major component (36.4%) in TEO. The bilayer films presented a well-integrated structure, with zein/TEO electrospun fibers showing uniform morphology, and FT-IR spectra confirmed efficient encapsulation. The films exhibited thermal stability, opacity with a slightly yellowish color, 0.194 mm thickness, low solubility, efficient water vapor barrier, suitable mechanical properties, low water contact angle, and biodegradation potential. Zein/TEO electrospun fibers presented a loading capacity of 33.2% and an encapsulation efficiency of 91.0%. The films demonstrated antioxidant activity and a high release rate of TEO. The bilayer design, combining polymers with electrospinning technology, is a promising approach that enables the integration of enhanced structural and bioactive functions, while maintaining biodegradability and suitability for sustainable food packaging. Future studies are recommended to evaluate its performance under real food storage conditions and to investigate its long-term stability.

Keywords *Ipomoea batatas* · L. · *Thymus vulgaris* · Electrospinning · Active food packaging

Introduction

Packaging is fundamental in the food industry, protecting food products from mechanical, chemical, and biological damage (Jacob et al., 2020). The development of food packaging films using renewable resources has garnered increasing attention, driven by evolving consumer demands and regulations focused on managing primary and post-consumer plastic waste (Nilsuwan et al., 2020). In this context, the production of biodegradable films has emerged as a promising alternative, facilitating the replacement of conventional polymers with environmentally friendly options for food packaging (Asgher et al., 2020).

Biopolymers, such as carbohydrates, have been widely researched for creating biodegradable and non-toxic films, mainly focusing on starch. Starch is frequently chosen as a starting material due to its film-forming capabilities, availability, high extraction yield, low cost, and biodegradability (Garavand et al., 2024; Luo et al., 2020). Native sweet potato starch (*Ipomoea batatas*, L.), an unconventional and easily cultivated source, offers a sustainable alternative to widely commercialized modified corn and cassava starches. With its high productivity and agricultural potential, sweet potato is a promising raw material for ecological packaging and industrial applications (Kolarič et al., 2020; Vannini et al., 2021).

However, materials produced from biopolymers still present limitations for use as food packaging, particularly due to their reduced mechanical properties and low efficiency as barriers to oxygen and moisture when compared to conventional synthetic packaging (Avila et al., 2023). Due to the hydrophilic nature of starch, especially after gelatinization, the structure of starch-based films is susceptible to

Extended author information available on the last page of the article

Published online: 01 August 2025

degradation in high-humidity environments and may become an inefficient barrier to water vapor (Frangopoulos et al., 2023; Sun et al., 2019). Previous studies have reported the limited barrier efficiency of sweet potato starch films (Ballesteros-Mártinez et al., 2020; Otero-Herrera et al., 2025). For instance, Ballesteros-Mártinez et al. (2020) found that even with the incorporation of various plasticizers at different concentrations, the films exhibited high water vapor permeability, highlighting the inherent structural limitations of the material.

The development of multilayer films has proven to be an effective strategy to overcome the limitations of biopolymer-based films by allowing the combination of different materials into a single functional structure (Nilsuwan et al., 2020; Souza et al., 2022). Ordoñez et al. (2022) demonstrated that the addition of a polyactic acid (PLA) layer containing cinnamic and ferulic acids enhanced the barrier properties of starch films by reducing their moisture sensitivity. Wang et al. (2020) employed a multilayer system produced by electrospinning, consisting of fibers capable of controlled curcumin release, with performance superior to monolayer gelatin films. Similarly, Estevez-Areco et al. (2020) developed bilayer films composed of thermoplastic starch and electrospun polyvinyl acetate (PVA) fibers containing antioxidant compounds, highlighting electrospinning as a promising technique for producing multilayer systems for food packaging. These approaches aim not only to improve the physical and functional properties of the films but also to facilitate the incorporation of natural active agents to extend shelf life and ensure food safety (Sedaghat Doost et al., 2020; Sogut & Seydim, 2019).

Essential oils, such as thyme (*Thymus vulgaris*), have attracted significant attention in the food industry due to their broad spectrum of biological activities. Their main active constituents, thymol and carvacrol, provide antibacterial, antifungal, and antioxidant properties (Galovičová et al., 2021). However, the aromatic nature of essential oils and their low stability under processing and environmental conditions, including heat, humidity, and oxygen, may restrict their application in food products (Mahanta et al., 2021; Moradi et al., 2023). A promising strategy to protect these compounds is their encapsulation in polymeric matrices, such as electrospun fibers, for subsequent incorporation into films (Reis et al., 2022).

Electrospinning is a simple and cost-effective technique that produces micro- or nanofibers at room temperature, preserving thermosensitive compounds. In active packaging, it enables controlled release, masks undesirable aromas, and protects active compounds from environmental stress (Rather et al., 2021). Zein, a hydrophobic protein derived from corn, is widely used as an encapsulating agent due to its biocompatibility, low moisture absorption, thermal stability, and oxygen barrier properties (Nanda et al., 2024; Pires et al., 2023; Wu et al., 2021). These characteristics enhance the stability and bioactivity of encapsulated compounds, contributing to extended food shelf life (Bumedi et al., 2023).

In this context, the development of bilayer films emerges as a promising approach by combining two complementary strategies: the incorporation and controlled release of essential oils and the enhancement of the limitations associated with conventional starch-based monolayer films. This trend is linked to the ability of such systems to optimize functional performance using a single packaging structure (Avila et al., 2023). Various methods and biopolymers have been employed in the production of these films (Avila et al., 2023; Chen et al., 2019; Ordoñez et al., 2022; Souza et al., 2022). Despite the extensive research on starch-based monolayer films, the literature currently lacks reports on starch films incorporating zein fibers loaded with essential oil. The combination of bio-based polymers, such as starch and zein, with electrospinning technology for the encapsulation of bioactive compounds into electrospun fibers represents an innovative and promising approach.

We hypothesize that the active bilayer material exhibits enhanced physicochemical properties compared to monolayer starch films, including greater thermal stability, improved water vapor barrier properties, adequate mechanical strength, and controlled release of the essential oil. This strategy offers a sustainable alternative for packaging, with the potential to contribute to food safety and shelf-life extension. Therefore, this study aimed to develop and characterize sweet potato starch bilayer films with an overlapping layer of zein electrospun fibers containing encapsulated thyme essential oil (TEO). The focus was to assess the feasibility of integrating two layers with distinct characteristics by analyzing their physicochemical, structural, mechanical, barrier, thermal, bioactive, and biodegradable properties, aiming at their application as active food packaging.

Material and methods

Material

The yellow sweet potato (*Ipomoea batatas* L. cv. Amelia) was acquired from the local market in Pelotas, Rio Grande do Sul, Brazil, for starch extraction. Glycerol (Labsynth, CAS 56–81-5, Brazil) was used to produce biodegradable films.

Thyme (*Thymus vulgaris*) essential oil was purchased from Ferquima (Indústria e Comércio de Óleos Essenciais, Brazil) in an amber bottle with a total volume of 100 mL (CAS 800–46-3, Sigma-Aldrich). Commercial zein was obtained from Sigma-Aldrich, Brazil (97% purity, CAS 9010–66-6), and ethanol (≥ 99.8% purity, Exodus Scientific, CAS 64–17-5), used as a solvent for the formation of electrospun fibers was acquired from Exodus Scientific. The MecLab MegaPurity® system provided ultrapure water (Milli-Q). Free radicals 2,2′-azino-bis(3-ethylbenzothiazoline) 6-sulfonic acid (ABTS; Sigma Aldrich, CAS 30931–67-0) and 2,2-diphenyl-1-picrylhydrazyl (DPPH; Sigma Aldrich, CAS 1898–66-4) were purchased from Sigma Aldrich.

Chemical composition of thyme essential oil by gas chromatography-mass spectrometry (GC-MS)

The TEO analysis was performed using a Shimadzu 2010 gas chromatograph equipped with an AOC-20i auto-injector and a Shimadzu MS-QP 2010 E mass selective detector (Shimadzu, Kyoto, Japan). The essential oil (10 µL) was dissolved in hexane (970 µL), and 1-nonanol internal standard (20 µL) (Sigma-Aldrich) was added. Then, 1 µL of the solution was injected. The sample preparation was performed according to the methodologies described by Torres et al. (2025) and Pires et al. (2024). A fused silica capillary column (Rxi-1MS, 100% dimethylpolysiloxane, non-polar stationary phase, 30 m × 0.32 mm × 0.25 µm; Restek®, USA) was employed for the chromatographic separation. The isothermal temperature programming followed the procedure by Pires et al. (2024). Compound identification was carried out by comparing the obtained mass spectra with the NIST (National Institute of Standards and Technology) mass spectral library. The concentration of individual compounds was determined relative to the internal standard 1-nonanol and by the relative percent peak area of TIC from the MS signal.

Extraction Process of Sweet Potato Starch

The starch was extracted following the method described by Cruz et al. (2023), with minor modifications. The potatoes were peeled and soaked in an aqueous solution of sodium metabisulfite ($Na_2S_2O_5$, 0.5% w/v, pH 5.0) for 15 min. The mixture was ground, filtered, and sieved (230 mesh, 63 µm), followed by successive washings. The filtered mass was allowed to settle, and the starch was decanted. The resulting starch was dried in an air-circulation oven at 40 °C for 24 h. After drying, the starch was ground into a fine powder and stored in an airtight container at room temperature (22 ± 2 °C). The extraction yield was 10.7%.

Films Preparation

Biodegradable starch films were prepared using the casting technique according to Fonseca et al. (2018). The suspension was prepared with 4.0% (w/v) starch in distilled water, with glycerol (Labsynth, CAS 56–81-5, Brazil) as a plasticizer at a plasticizer-to-starch ratio of 0.30 (g/g). These parameters were adopted based on previous tests and studies that demonstrated the effectiveness of producing starch films using this starch concentration and glycerol (Mao et al., 2023; Wu et al., 2023). The suspension was heated on a hotplate (FISATOM, 752 A, Brazil) with magnetic stirring at 90 °C for 30 min to achieve complete starch gelatinization. The suspension was then cooled to 50 °C, and 55.55 g were poured onto acrylic plates (Ø 15 cm) and dried in an oven (Ethik Technology, Brazil) with air circulation at 30 °C for approximately 16 h.

Production of Electrospun Fibers

Preparation and Characterization of the Polymer Solution

As defined in preliminary tests, the polymer solutions were prepared with 30% (w/v) zein in 70% ethanol (v/v, in Milli-Q water) as solvent. First, the solutions were stirred for 30 min in a magnetic stirrer to complete homogenization at room temperature (22 ± 2 °C). Then, TEO was incorporated into the zein solution at a concentration of 60% (v/w) and stirred for 15 min under dark conditions. The TEO concentration was selected based on a previous study by (Peixoto et al., 2023) and feasibility tests, aiming to incorporate the highest possible amount of essential oil without compromising the fiber structure. Finally, a solution without incorporating TEO was prepared as a control (Böhmer-Maas et al., 2020).

The viscosity and electrical conductivity parameters were evaluated to characterize the polymer solutions. The apparent viscosity was evaluated using a Brookfield digital viscometer (Model DV – II, USA) equipped with an SC4-18 spindle. Approximately 10 mL of each solution was placed in a stainless-steel sample chamber for analysis. The electrical conductivity of the solutions was determined using a conductivity meter (model CON500, Benchtop Meter, USA) and expressed in µS/cm. All measurements were made at room temperature (23 ± 2 °C) in triplicate (Silva et al., 2018).

Electrospinning Process

The electrospun fibers were produced according to the method of Peixoto et al. (2023), with modifications. The polymer solutions were placed in a 10-mL disposable syringe

fitted with a needle with an inner diameter of 0.8 mm at 20 cm from the needle to the fibers' collector. Then, the polymer solution was pumped with a flow rate of 0.9 mL/h for 11 h by an infusion pump (KD Scientific, Model 100, Holliston, England) under a system voltage of 20 kV (Instor, INSES-HV30, Brazil), to deposit 10 mL of the solution, forming a homogeneous fiber layer that fully covered the surface of the starch film. The collector was coated with aluminum foil to facilitate the removal of fibers after the electrospinning process was completed under controlled temperature (18 ± 2 °C) and relative humidity (40 ± 2%) using an air conditioner and a dehumidifier, respectively. The same procedure was performed to collect the electrospun fibers directly on the starch films fixed to the collector, forming a bilayer film.

Characterization of Films, Electrospun Fibers, and Bilayer Films

The materials produced and characterized are referred to throughout the text as follows: zein fibers (electrospun pure zein fibers), zein/TEO fibers (electrospun zein fibers with encapsulated TEO), starch films (single-layer films composed of starch and glycerol), bilayer film with zein fibers (bilayer starch films with pure zein fibers), and bilayer film with zein/TEO fibers (bilayer starch films with TEO-loaded zein fibers).

Morphology

The morphology of the starch film, zein fibers, and bilayer films with and without TEO was evaluated by scanning electron microscopy (SEM, Jeol, JSM–6610LV, NJ, USA) (Fonseca et al., 2020). For cross-sectional micrographs, the films were fractured using liquid nitrogen and then placed in a stub; while for surface micrographs, the films were cut and similarly mounted on stubs. The samples were coated with gold using a sputter (Desk V, JEOL, USA). The cross-section and surface micrographs were visualized using an accelerating voltage of 10 kV.

The mean diameter and size distribution of the fibers were assessed based on a random measurement of 60 fibers using ImageJ software (version 2015, USA) for the images produced by SEM.

Absorption Profile in FT-IR Infrared

The functional groups present in TEO, starch film, zein fibers, and bilayer films were evaluated by FT-IR spectrometry (Karim et al., 2020). A Fourier transform infrared spectrum 100 FT-IR spectrometer (PerkinElmer, USA) equipped with a zinc selenide crystal and set to a resolution of 4000–500 cm^{-1}. A sufficient sample was added to cover the equipment crystal, and 32 scans were performed.

Thermal Properties

For thermogravimetric analysis, approximately 5 mg of each sample was individually placed in platinum capsules. The analysis used a TG-60 instrument (Shimadzu, Kyoto, Japan) under a nitrogen atmosphere with a flow rate of 50 mL/min. The samples were heated from 30 to 500 °C at a constant heating rate of 10 °C/min. An empty platinum plate was used as a reference (Lancuški et al., 2017). The data were processed using TA-60WS software (version 2.20, Shimadzu Corporation, Japan). The weight loss was calculated using Eq. (1). Where W_i is the initial weight of the sample and W_f is the final weight of the sample at each temperature.

$$Weight\ loss = \left(100 - \left(\frac{W_i - W_f}{W_i}\right)\right) \times 100 \quad (1)$$

Color

The color and opacity of the films were evaluated by averaging five measurements obtained from each sample in triplicate using a colorimeter (3nh, NR 200, China), following the method described by do Evangelho et al. (2019). The films were placed on a white plate set as the standard to determine the color parameters with illuminant D65 (daylight). The parameter L* represents luminosity, ranging from 0 (black) to 100 (white); the parameters a* and b* are the chromaticity coordinates, where a* ranges from green (-) to red (+), and b* ranges from blue (−) to yellow (+). The total color difference (ΔE*) was calculated using Eq. (2), where $\Delta L^* = L_{\text{white standard}} - L_{\text{sample}}$; $\Delta a^* = a_{\text{white standard}} — a_{\text{sample}}$; $\Delta b^* = b_{\text{white standard}} - b_{\text{sample}}$.

$$\triangle E^* = \sqrt{(\triangle L^*)^2 + (\triangle a^*)^2 + (\triangle b^*)^2} \quad (2)$$

Opacity was calculated as the relation between the opacity of the film (parameter "y") superimposed on the black standard (S_{black}) and the white standard (S_{white}), according to Eq. (3).

$$\text{Opacity} = \frac{S_{\text{black}}}{S_{\text{white}}} \times 100 \quad (3)$$

Moisture Content and Solubility in Water

The moisture content of the films was determined following the method described by do Evangelho et al. (2019). The films were dried in an oven at 105 °C for 8 h with air circulation until a constant mass was achieved, and the results were expressed in g/100.

The solubility of the films in water was evaluated through immersion assays. Samples were immersed in 50 mL of distilled water under constant shaking for 24 h at 25 °C. After immersion, the films were collected and dried at 110 °C until reaching a constant weight (W_f), and their solubility in water (%) was calculated using the following Eq. (4), where *Wi* is the initial dry weight of the film.

$$Solubility\ in\ water\ \% = \frac{W^i - W^f}{W^i} \times 100 \quad (4)$$

Water Vapor Permeability

The water vapor permeability (WVP) of the starch films and the bilayer films was determined by the gravimetric method E96-95-ASTM (ASTM, 1995). Film samples were sealed with industrial standard sealing lubricant (MOLYKOTE®, Dow Corning Corporation, Germany) in aluminum permeation cells containing pre-dried (0% relative humidity) calcium chloride ($CaCl_2$) anhydrous salt. Films were stored at 23 ± 2 °C and 50% ± 5% of relative humidity.

The increase in the mass of the system, resulting from water transfer through the sample, was monitored at regular 24-h intervals. The WVP was calculated (Eq. 5) with the slope of the linear regression from the weight gain over time in the constant rate period, normalized by the film exposed area. The difference in partial vapor pressure between the two sides of the films was 1406 Pa (50% relative humidity and saturation vapor pressure at 23 °C equal to 2812 Pa).

$$WVP = \frac{\triangle_W}{t} \times \frac{X}{A\triangle_P} \quad (5)$$

where WVP is the water vapor permeability (g.mm/m^2.day. Kpa), Δ_W is the absorbed moisture mass (g), t is the incubation period time (days), X is the film thickness (mm), A is the exposed film surface area (m^2), and Δ_P is the difference of partial pressure trough the film (Pa).

Mechanical Properties

The thickness of the starch films and the bilayer films was measured using a digital micrometer (MI20 Adamel Lhomargy, France) with an accuracy of 0.001 mm. Thickness was measured in triplicate, and five random positions around the film were measured in each triplicate. The average values were used in film evaluation calculations (Fonseca et al., 2018).

The mechanical properties of the films were determined using a texturometer (TA.XT plusC—Texture Analyser, Stable Micro Systems, UK), evaluating the tensile strength, percentage of elongation at break, and adhesiveness, operating according to the ASTM D-882–10 method (ASTM, 2010). The tensile strength and elongation at break were measured with an initial grip separation of 40 mm and a probe speed of 0.8 mm/s. The films were cut (85 mm × 25 mm) and fixed in the probe in the texturometer. Seven measurements were conducted on each sample. The tensile strength was calculated by Eq. (6), where *TS* is tensile strength (MPa), F_m is the maximum force at the moment of film rupture (N), and A is the cross-sectional area (m^2) and elongation by Eq. (7), where E is elongation (%); d_i is the initial separation distance (cm), and d_r is the distance at the moment of rupture (cm).

$$TS = \left(\frac{F_m}{A}\right) \quad (6)$$

$$E = \left(\frac{d_r}{d_i}\right) \times 100 \quad (7)$$

The adhesiveness of the films was measured using a 1-cm diameter film sample that was placed on the fixed metal surface of the equipment and pressed with a metal plate featuring a 6-mm diameter cavity in the middle, exposing a portion of the film. A probe with a 19.63 mm^2 contact area was attached to the metal support on top of the texture analyzer. During contact, a force of 200 g was applied, with a contact time of 15 s and a test speed of 0.5 mm/s. The texture analyzer lowered the probe until it pressed against the film surface, then raised it after 15 s, measuring the force required to tear the film from the surface. This analysis was repeated eight times for each film treatment.

Contact Angle

The water contact angle (wettability) of the starch film, zein fibers, and bilayer films was evaluated following the methodology described by Böhmer-Maas et al. (2020). Samples were deposited on glass slides, and measurements were performed at room temperature using an optical tensiometer (Theta Lite Model TL100, BiolinScientific, Sweden), and the readings were recorded using the OneAttension software (BiolinScientific, Sweden). For analysis, a drop of distilled water (3 µL) was dripped onto the surface of the sample. The contact angle with water and the time for water absorption were captured using a digital camera.

Biodegradability

The biodegradability of the films was evaluated following the EN 13432 and ASTM D-6400 standards (ASTM, 2023). Plastic trays with dimensions of 30 × 40 × 15 cm were used, filled uniformly with commercial compost (soil) (Universal Biological Substrate, Portugal) up to a height of 5 cm. Film samples measuring 3 × 3 cm were weighed to record their initial weight (M_i). Subsequently, the samples were buried and covered with an additional 3 cm layer of compost.

The test conditions were maintained at a constant temperature of 60 °C and 50% relative humidity (RH), monitored over 35 days. Weekly, duplicates of each treatment were carefully dug up and photographed, and adhering compost was removed for analysis. The mass loss of the samples was recorded, and the visual degradation of the films was monitored. The degradation percentage was calculated using the following Eq. (8), where *Mi* is the weight of films at an initial time, and M_f is the weight of films at different times (1st, 7th, 14th, 21 st, 28th, and 35th day).

$$Degradation\ (\%) = \frac{M_i - M_f}{M_i} \times 100 \tag{8}$$

Loading Capacity (LC) and Encapsulation Efficiency (EE) of Zein Electrospun Fibers

With adaptations, the LC and EE were determined as per Valizadeh et al. (2024). The content of external TEO compounds was quantified by weighing 40 mg of fibers and gently agitating with 2 mL of hexane. The mixture was then centrifuged at 3226 × *g* for 5 min. The resulting supernatant was collected and analyzed using a spectrophotometer at 725 nm. To determine the total content of TEO compounds (due to fiber rupture), 40 mg of fibers were agitated for 2 min with 250 µL of 70% ethanol. After complete fiber rupture, 1750 µL of hexane was added for complete homogenization, and the mixture was centrifuged (Eppendorf 5430 R Centrifuge, Germany) at 3226 × *g* for 5 min. The supernatant was collected and analyzed using a UV–Vis spectrophotometer (Tecnal UV-5100 model, Metash Shanghai, China) at 725 nm, employing a calibration curve of TEO. For this, different concentrations of thyme EO (ranging from 0.01 to 0.1 mg/mL) were dissolved in hexane, and the absorbance of the solutions was measured at 725 nm. The LC and EE of the electrospun zein fibers were calculated using Eqs. (9) and (10), where W_1 is the content of TEO compounds in the solution (external washing of the fibers, without rupture), W_2 is the total content of TEO compounds (internal and external—due to fiber rupture), and M is the total content of TEO compounds estimated in the fibers.

$$LC\ (\%) = \frac{W_2}{M} \times 100\% \tag{9}$$

$$EE(\%) = \frac{W_2 - W_1}{W_2} \times 100\% \tag{10}$$

In Vitro Release of TEO from Zein Electrospun Fibers

The release of TEO compounds from electrospun zein fibers was conducted in 10% ethanol (hydrophilic), 50% ethanol (lipophilic), and hexane (highly hydrophobic). These media simulate food products with high water content (hydrophilic) and fatty foods (hydrophobic). The ethanol-based media were selected as food simulants, as established by the Commission Regulation 10/2011 EU. Hexane was chosen as a highly hydrophobic medium to assess the efficiency of the encapsulating polymer matrix in promoting a controlled release of the lipophilic essential oil compounds while being compatible with the GC–MS analytical system.

The release assay was performed at room temperature (22 ± 5 °C), following the methodology adopted by Fonseca et al. (2020). The electrospun fibers (150 mg) were immersed in each of the aforementioned media (5 mL), and the release kinetics of the essential oil were calculated over 48 h. At each time interval (1 h, 2 h, 3 h, 4 h, 5 h, 12 h, 24 h, and 48 h), 0.3-mL aliquots were withdrawn and mixed with 0.7 mL of hexane. After centrifugation of the resulting mixture at 3226 × *g* for 2 min, the supernatant was analyzed using the GC–MS (as described in the "Chemical Composition of Thyme Essential Oil by Gas Chromatography-Mass Spectrometry" section) to determine the concentration of the released compounds.

Antioxidant Activity

The *in vitro* antioxidant activity of TEO, starch film, zein fibers, and bilayer films was performed individually using 1 mg of each sample. For the ABTS (2,2′-azino-bis(3-ethylbenzothiazoline) 6-sulfonic acid) radical scavenging assay, 3 mL of ABTS solution was added to the samples, which were then stirred for 1 min and kept in the dark for 30 min. Absorbance was subsequently measured at 734 nm, following the method proposed by (Re et al., 1999). For the DPPH (2,2-diphenyl-1-picrylhydra + zyl) radical scavenging assay, 3.9 mL of DPPH solution was added to the samples, stirred for 1 min, and kept in the dark for 2 h and 30 min. Absorbance was then measured at 515 nm, according to the method described by Brand-Williams et al. (1995).

The results were expressed as a percentage (%) of radical inhibition and calculated using Eq. (11), where A_c is the

absorbance of the reaction without the sample and A_s is the absorbance of the reaction with the sample.

$$Inhibition\ (\%) = \frac{A_c - A_s}{A_c} \times 100 \quad (11)$$

Statistical Analysis

All analytical determinations were conducted in at least triplicate, and the results were expressed as means ± standard deviations. Statistical analysis was performed using analysis of variance (ANOVA), followed by Tukey's test to compare means. Differences were considered statistically significant at a threshold of $p < 0.05$.

Results and Discussion

Chemical Composition of TEO by Gas Chromatography-Mass Spectrometry

The components of TEO identified by GC/MS are listed in Table 1. *p*-cymene was identified as the major component (36.46%), followed by thymol (29.48%), carvacrol (5.78%), γ-terpinene (5.34%), linalool (4.63%), α-pinene (3.49%), D-limonene (2.80%), camphene (1.99%), β-myrcene (1.21%), eucalyptol (1.18%), borneol (1.12%), β-pinene (0.31%), α-phellandrene (0.16%), and p-menthane, cis- (0.08%). In total, 14 compounds were identified by GC/MS (Table 1 and Supplementary material 1). Previous studies have reported a similar qualitative chemical composition for the major constituents of TEO, including thymol (23–60%), γ-terpinene (18–50%), *p*-cymene (8–44%), carvacrol (2–8%), and linalool (3–4%), albeit with variations in concentrations (Satyal et al., 2016). Compounds such as thymol, γ-terpinene, and *p*-cymene have demonstrated potent antioxidant and antibacterial properties, significantly contributing to the biological activities of TEO (Dong et al., 2023), which makes this essential oil appealing for applications such as food product preservation.

Viscosity and Electrical Conductivity

The zein solutions (30%, w/v), pure and with TEO (60%, v/w), used to produce the electrospun fibers had an average viscosity of 59.11 and 66.5 mPa/s, respectively (Table 2). This indicates that the presence of zein in ethanol in the solutions provides adequate viscosity for the formation of fibers, which increases with the presence of TEO. The increase in viscosity upon adding the essential oil to the polymeric solution was also reported by Antunes et al. (2017) when incorporating a complex with eucalyptus essential oil (24% w/v) in a zein solution (30% w/v). This effect can be explained by the ability of zein to form interactions with the hydrophobic compounds present in the TEO, resulting in the formation of a denser network and an increase in the solution's resistance to flow. This results in sufficient chain entanglement with strong viscoelastic forces that resist axial stretching during electrospinning, leading to fibers with the mentioned characteristics (Nanda et al., 2024).

However, the presence of TEO decreased the electrical conductivity of the polymer solution from 1261.66 to 1034 µS/cm. This is likely due to the increase in viscosity, which created a denser network, restricting the mobility of charged particles (ions) within the solution (Nanda et al., 2024). According to Azizi et al. (2023), for the electrospinning process to occur, the polymer solution must acquire sufficient

Table 1 Chemical composition of thyme essential oil

No	*RT (min)	Compound name	Class	Formula	%	mg/mL		
1	3.122	*α*-Pinene	Monoterpene	$C_{10}H_{16}$	3.49	38.00	±	0.20
2	3.303	Camphene	Monoterpene	$C_{10}H_{16}$	1.99	21.64	±	0.13
3	3.731	*β*-Pinene	Monoterpene	$C_{10}H_{16}$	0.31	3.32	±	0.02
4	3.806	*p*-Menthane, cis-	Monoterpene	$C_{10}H_{20}$	0.08	0.89	±	0.01
5	4.001	*β*-Myrcene	Monoterpene	$C_{10}H_{16}$	1.21	13.17	±	0.07
6	4.210	*α*-Phellandrene	Monoterpene	$C_{10}H_{16}$	0.16	1.75	±	0.01
7	4.501	*p*-Cymene	Monoterpene	$C_{10}H_{14}$	36.46	396.70	±	2.27
8	4.634	Eucalyptol	Monoterpene oxygenated	$C_{10}H_{18}O$	1.18	12.85	±	0.33
9	4.687	D-Limonene	Monoterpene	$C_{10}H_{16}$	2.80	30.50	±	0.14
10	5.275	*γ*-Terpinene	Monoterpene	$C_{10}H_{16}$	5.34	58.09	±	0.32
11	6.104	Linalool	Monoterpene oxygenated	$C_{10}H_{18}O$	4.63	50.39	±	0.12
12	7.493	Borneol	Monoterpene oxygenated	$C_{10}H_{18}O$	1.12	12.15	±	0.08
13	10.826	Thymol	Monoterpene phenol	$C_{10}H_{14}O$	29.48	320.69	±	5.90
14	11.050	Carvacrol	Monoterpene phenol	$C_{10}H_{14}O$	5.78	62.87	±	0.10

**RT* Retention time (min); (%) = percentage of compounds in the essential oil

electrostatic charge for the repulsive force to overcome the surface tension. Moreover, the jet elongation depends on the solution's ability to conduct these charges, which facilitates the continuous stretching of the fluid until fiber formation.

Morphology

Figure 1 illustrates the morphology and size distribution of fibers, both with and without TEO, as well as their application on starch films. The zein fibers produced with encapsulated TEO exhibited a cylindrical, homogeneous, and continuous morphology without the presence of droplets or beads (Fig. 1(2a)). However, the zein fibers without essential oil displayed a flatter morphology, characterized as ribbon-like, with some fused fibers and no beads (Fig. 1(1a)).

According to Bhardwaj and Kundu (2010), the appropriate viscosity of the polymer solution used in the electrospinning process is one of the key factors that enables the formation of continuous, uniform fibers without beads. However, as noted by Heydari-Majd et al. (2019), pure zein fibers tend to exhibit a ribbon-like structure. This is attributed to the formation of β-structures, composed of polypeptide chains aligned side by side and stabilized by hydrogen bonds, which do not fully expand. This behavior occurs due to the rapid evaporation of ethanol during the electrospinning process, which prevents the proper reorganization of polymer chains within the fibers. The accelerated solvent evaporation restricts the mobility of zein chains, leading to the formation of these characteristic flat structures.

Studies conducted by Hosseini et al. (2021) and Ghasemi et al. (2022) reported an increase in the diameter of the fibers with higher concentrations of essential oils (rosemary and cumin, respectively), which leads to a decrease in electrical conductivity and an increase in viscosity. It is known that during the electrospinning process, the morphology of the fibers is strongly influenced by various parameters, such as polymer concentration and type, needle-to-collector distance, solution flow rate, applied voltage, and others (Azizi et al., 2023; Heydari-Majd et al., 2019). However, in the present study, contrary to expectations, the addition of TEO to the polymer solution resulted in a significant decrease in the diameter of the fibers (Fig. 1(1b, 2b, 4b, and 5b)).

Pure zein electrospun fibers exhibited an average diameter of 579.88 nm, ranging from 332 to 934 nm, with a significant difference between those collected directly on the starch film (636 nm) and those collected on the target collector (523 nm). Heydari-Majd et al. (2019) reported similar values when producing 35% (w/v) zein fibers in an ethanol solution with an average diameter of 724 nm. In the present study, the addition of TEO to the zein solution resulted in fibers with a significantly smaller average diameter of 376 nm, ranging from 228 to 661 nm, with no significant difference between those collected directly on the starch film (362 nm) and those collected on the target collector (391 nm), being classified as ultrafine fibers. Antunes et al. (2017), when encapsulating a β-cyclodextrin and eucalyptus essential oil complex in zein fibers, observed no correlation between the percentage of encapsulated essential oil and the average diameter of the resulting fibers.

In this study, the reduction in fibers' diameter can be attributed to the synergy among the hydrophobic compounds present in the polymer solution. Zein, being a predominantly hydrophobic protein, exhibits high compatibility with TEO, whose main components, such as thymol and carvacrol, are also hydrophobic (Garavand et al., 2024; Rezaei et al., 2019). This chemical affinity facilitates a more homogeneous dispersion of the components, preventing aggregate formation and promoting better jet stability during electrospinning. As a result, this interaction contributes to the formation of thinner and more uniform fibers, enhancing the mechanical and structural properties of the fibers (Nanda et al., 2024). Therefore, the combination of zein with TEO had a positive effect on the morphology of the electrospun fibers, allowing for a significant reduction in average diameter. These characteristics were maintained even when the fibers were collected on starch films, indicating that the use of film substrates on the collector target did not cause morphological changes in the fibers.

The surface and cross-sectional morphology of the sweet potato starch film (Fig. 1(3a and 3b)), the bilayer starch film with zein electrospun fibers (Fig. 1(4a and 4c)), and the bilayer starch film with zein/TEO electrospun fibers (Fig. 1(5a and 5c)) were illustrated through micrographs. The starch film exhibited a continuous and homogeneous

Table 2 Polymer solution properties (apparent viscosity and electrical conductivity) and performance (loading capacity and encapsulation efficiency) of zein electrospun fibers

Zein (% w/v)	TEO (% v/w)*	Apparent viscosity (mPa/s)	Electric conductivity (μS/cm)	Loading capacity (%)	Encapsulation efficiency (%)
30	0	59.11 ± 0.12^{b}	1261.66 ± 3.51^{a}		
30	60	66.50 ± 0.20^{a}	1034.00 ± 1.52^{b}	$33.2\% \pm 4.41$	$91.0\% \pm 1.20$

The results are expressed as the mean ($n = 3$) ± standard deviation. [a,b]Different letters in the same column differ statistically ($p < 0.05$). *TEO:Thyme essential oil

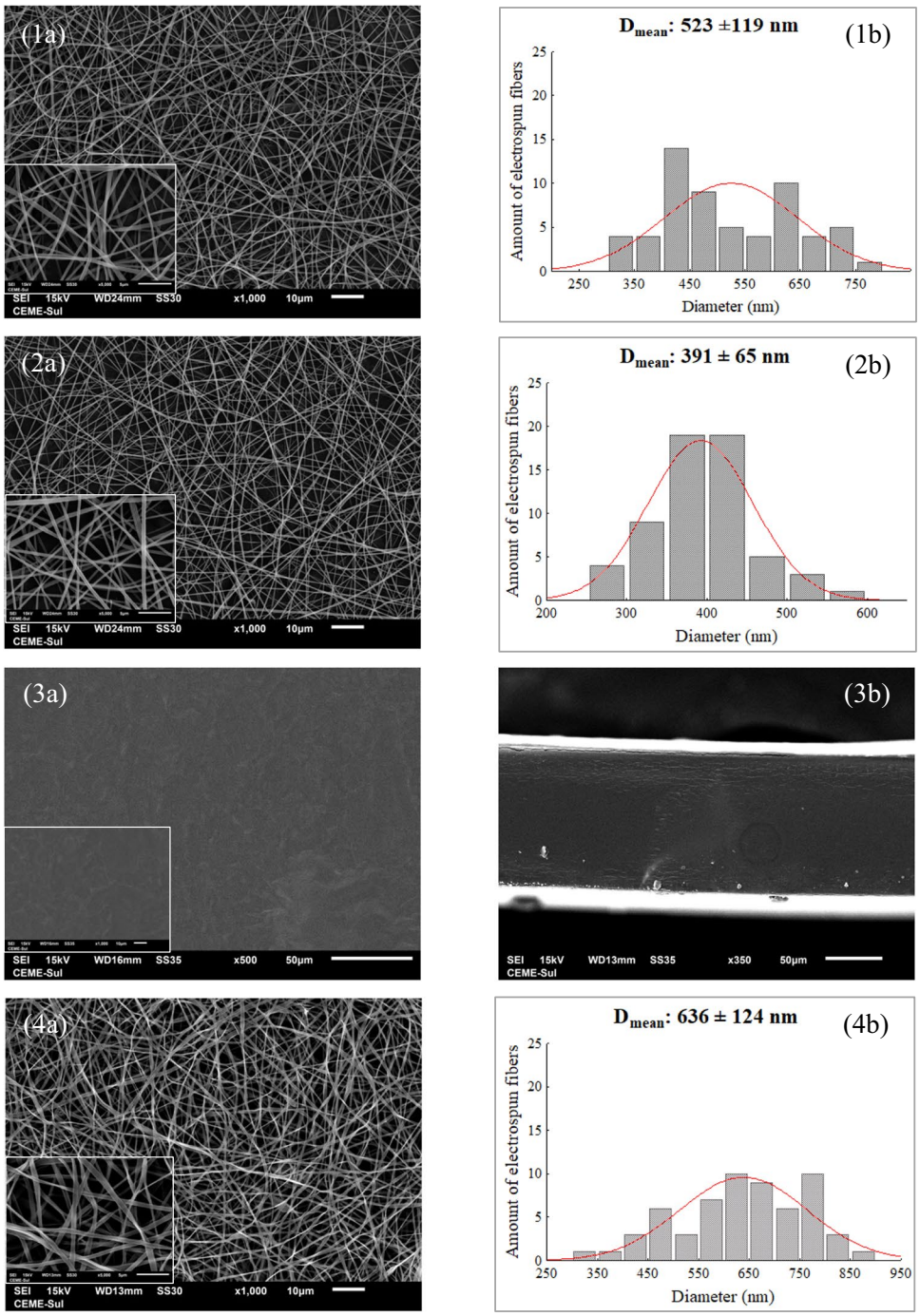

Fig. 1 Morphology and size distribution of the zein fibers (1a, 1b), zein/TEO fibers (2a, 2b), starch film (3a, 3b), bilayer film with zein fibers (4a, 4b, 4c), and bilayer film with zein/TEO fibers (5a, 5b, 5c)

surface with nearly imperceptible alterations, a characteristic associated with proper starch gelatinization (Cheng et al., 2021). These features were confirmed by the cross-sectional micrograph, which displayed a smooth structure free of cracks or porosity. The morphology of the films can be influenced by the botanical source of the starch and the plasticizer concentration (Song et al., 2021). However, Basiak et al. (2017), Guo et al. (2021), and Evangelho et al. (2019) reported similar results for starch-based films containing glycerol content ranging from 15 to 30% of the dry matter.

In the surface micrographs of bilayer starch films with zein electrospun fibers (Fig. 1(4a and 5a)), the morphological characteristics of the films are not visible, as the fibers entirely cover the material's surface densely and continuously. In the cross-sectional micrographs (Fig. 1(4c and 5c)), a closely integrated double-layer structure can be observed,

Fig. 1 (continued)

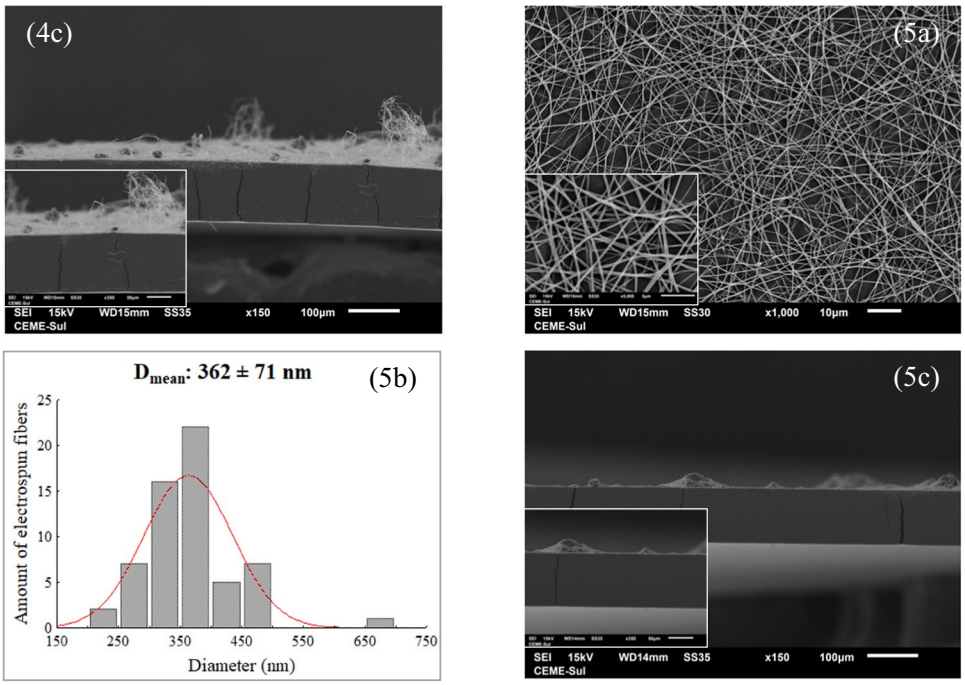

formed by the deposition of fibers onto the film surface, suggesting good compatibility between the layers.

However, the presence of some cracks can be observed, possibly attributed to temperature and humidity variations during the electrospinning process, where the starch films were exposed to conditions different from those applied to pure starch films. Additionally, the deposition of zein electrospun fibers may have disrupted the moisture equilibrium at the film interface, promoting localized drying and contributing to the formation of cracks. Morphological changes in the production of bilayer films have also been reported by Reddy et al. (2018). The authors demonstrated that incorporating cellulose nanofibers onto the surface of glycerol-plasticized starch films, which were initially smooth, led to an increase in surface roughness.

Fourier Transform Infrared Spectroscopy

In the Fourier transform infrared (FT-IR) analysis, characteristic bands of the raw materials used to produce the films (starch) and fibers (zein), as well as the encapsulated bioactive compound (TEO), can be observed (Fig. 2a).

TEO contains *p*-cymene, thymol, carvacrol, γ-terpinene, and linalool, among other major compounds previously reported in the "Chemical Composition of TEO by Gas Chromatography-Mass Spectrometry" section. In the infrared region of the spectroscopy, characteristic bands of these compounds were observed at 2960, 2930, and 2872 cm^{-1}, corresponding to the symmetric (νs C-H) and asymmetric (νa C-H) vibrations of C-H bonds, representing sp^3 and sp^2 hybridizations present in the structures of the mentioned compounds. Additionally, a band at 1516 cm^{-1} (νC = C) was observed, associated with the aromatic rings in thymol, p-cymene, and carvacrol; bands at 1447 cm^{-1} (νC-C) and 1417 cm^{-1} (νC-O), corresponding to the phenyl group in thymol; and a band at 807 cm^{-1} (γC-H), characteristic of isoprenoid compounds, similar to findings reported in other studies (Ardjoum et al., 2021; Fonseca et al., 2020; Peixoto et al., 2023; Radünz et al., 2020).

In zein, as well as in the zein fibers (Fig. 2b), bands around 3291, 1642, and 1522 cm^{-1} were identified, indicating the presence of amide I (C = O stretching) and amide II (C—N stretching adjacent to N–H bending), respectively. This was expected because this region serves as a fingerprint for proteins such as zein, a prolamin extracted from corn. The bands between 2872 and 2958 cm^{-1} are related to the C—H bond stretching observed in all spectra, which is a characteristic of zein's structure (Bruni et al., 2020; Silva et al., 2018).

Sweet potato starch and starch films exhibited characteristic bands at 3304 cm^{-1} (νO-H), attributed to inter- and intramolecular hydroxyl groups between amylose chains, and at 2927–2888 and 2800 cm^{-1} (νsC-H; νaC-H) from the cyclic chain (Fonseca et al., 2020). The spectra showed absorption bands at 1642, 1420, and 1148 cm^{-1} corresponding to hydrogen bonding in the amorphous region of the granules (δOH), amylopectin (δsCH$_2$), and the alpha-1,4 glycosidic bond (νasC–O–C). Molecular chain bands were also observed at 1077 cm^{-1} (νC–O), 996 cm^{-1} (νO–C–C), 927 cm^{-1} (νC–OH), and 858 cm^{-1} (δCH$_2$). All these groups

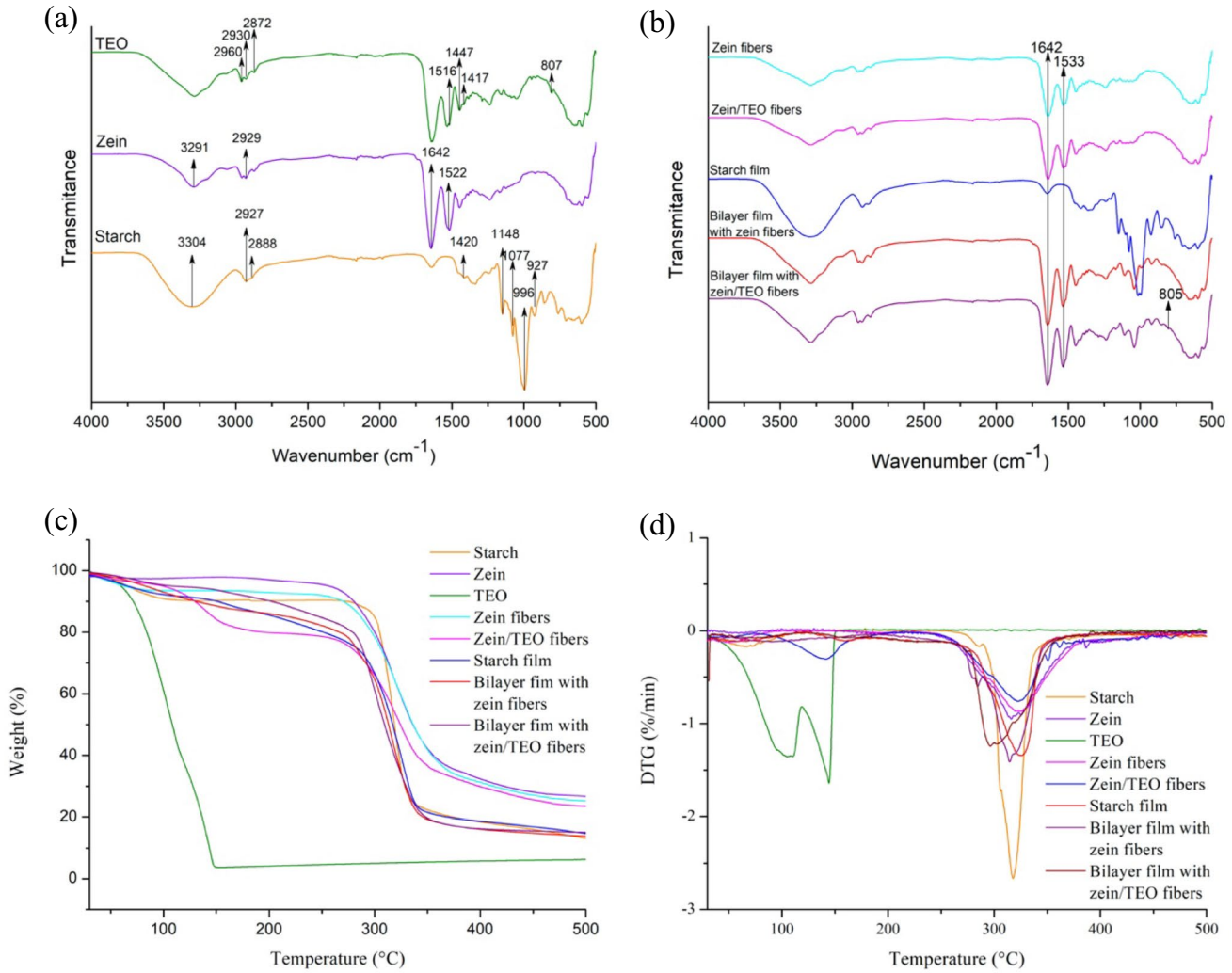

Fig. 2 FTIR spectra (**a**, **b**), thermograms (**c**), and their first derived (derivative thermogravimetry) (**d**) of the thyme essential oil (TEO), zein, sweet potato starch, zein fibers, zein/TEO fibers, starch film, bilayer film with zein fibers, and bilayer film with zein/TEO fibers

are present in the structures of starch and glycerol, which are used in the formation of the films (Cruz et al., 2023; Guimarães et al., 2024).

The zein fibers with encapsulated TEO exhibited the same characteristic bands as the fibers without TEO. No differences were observed between the bands of the electrospun fibers, regardless of TEO incorporation, except for the 807 cm^{-1} band, which was found with low intensity in the compounds containing TEO. This suggests a loading capacity of the electrospun fibers that interact with TEO as an encapsulating material or a possible overlap of peaks.

Thermogravimetric Analysis

The thermogravimetric analysis (TG) and its first derivatives were performed to investigate the thermal degradation of the bilayer films and their components (Fig. 2c and Table 3). The derivative thermogravimetry (DTG) provided the first derivative of the TG curve as a function of temperature (Fig. 2d).

From the DTG analysis, it was observed that sweet potato starch exhibited a mass loss in two stages: the first stage showed a mass loss (Δm_1) of ~ 8.7%, with a peak temperature (T_{p1}) of ~ 66.6 °C, corresponding to the elimination of volatile compounds and dehydration of the starch. The second stage showed Δm_2 of ~ 71.6% at T_{p2} of ~ 317.8 °C, which is attributed to the disintegration and thermal decomposition of the starch (Cruz et al., 2023). Zein exhibited only one peak with Δm_1 of ~ 68.7% at T_{p1} of ~ 318.9 °C, which is associated with protein degradation and peptide bond cleavage (Bruni et al., 2020). It was observed that TEO degraded within a temperature range of ~ 32.7–161.5 °C and showed two peaks, with Δm_1 of ~ 61.5% at T_{p1} of ~ 106.1 °C and Δm_2

of 32.8% at T_{p2} of ~ 144 °C, due to the loss of volatile compounds and decomposition of TEO (Fonseca et al., 2020).

The zein fibers loaded with TEO exhibited a mass loss in three stages. The first and last stages were similar to those observed for pure zein fibers, while the second stage showed a Δm_2 of approximately 16.6% with T_{p2} around 140.4 °C, a temperature close to that of TEO but with a smaller mass loss. This behavior in the second stage may be associated with the degradation of TEO, which occurs with lower intensity when encapsulated in zein fibers. The encapsulation of bioactive compounds via electrospinning is a promising approach, as this process enhances the thermal stability of the compounds and enables the development of packaging with improved properties (Bruni et al., 2020).

The starch films, whether pure or bilayer, showed two thermal peaks in similar temperature ranges. The first peak, with Δm_1 ranging from ~ 4.2 to ~ 11.5% and T_{p1} between ~ 60.3 and ~ 85 °C, was attributed to water evaporation. The second peak, with Δm_1 ranging from ~ 63.8 to ~ 70.2% and T_{p2} between ~ 298.8 and ~ 325.5 °C, was associated with the thermal degradation of the compounds present, including glycerol (Basiak et al., 2017). Although these values are similar to those observed for pure starch, which can be attributed to the predominance of starch in the formulation, the incorporation of glycerol may have influenced the thermal properties of the films. The presence of the plasticizer tends to anticipate the onset of thermal degradation of the polymer matrix, slightly lowering the temperature of the second degradation stage, likely due to reduced intermolecular interactions between starch chains. This plasticizing effect increases molecular mobility, facilitating the thermal breakdown of bonds (Basiak et al., 2017; Nordin et al., 2020). These findings suggest that while glycerol is essential for improving the mechanical properties of the films, it may also compromise their thermal stability, which is a critical factor for applications requiring heat resistance (Ballesteros-Mártinez et al., 2020).

Color

The color parameters (L^*, a^*, b^*, and ΔE) and opacity of the starch films and the bilayer films are described in Table 4. The brightness (L) of the films varied significantly ($p < 0.05$) from 89.70 to 97.28, indicating high luminosity, as the values were close to 100. The chromaticity coordinates (a^* and b^*) showed a tendency for neutral and yellowish tones in the pure starch films. In the bilayer films, a trend towards greenish and yellowish hues was observed. As the compounds were added, the b^* values increased, indicating a more intense yellow color. This behavior was expected due to the characteristic hue of zein and TEO (Chen et al., 2019). Hou et al. (2024) reported that as the TEO concentration increases, the ΔE and b^* values increase, while the L^* and a^* values decrease.

In this study, the total chromatic difference (ΔE) values ranged from 1.63 to 12.49, with bilayer films containing pure zein fibers showing the highest difference. In contrast, the starch films without fibers exhibited the smallest differences. As found by Basiak et al. (2017), pure sweet potato starch films showed low opacity at 8.6%. The opacity of the films increased with the incorporation of new compounds on the surface. As expected, the bilayer films containing zein/TEO fibers exhibited 95.9% opacity. This increase occurs because the deposition of fibers with TEO forms a layer on the film's surface, creating an irregular interface that intensifies light scattering. Additionally, the incorporation of fibers contributes to the increase in film thickness; thicker layers allow less light to pass through, resulting in higher opacity (Basiak et al., 2017). The presence of natural pigments, such as those intrinsic to zein and TEO, also absorbs some visible

Table 3 Thermogravimetric properties of starch, zein, TEO, zein fibers, zein/TEO fibers, starch film, bilayer film with zein fibers, and bilayer film with zein/TEO fibers

Sample	Thermogravimetric properties*											
	T_{01} (°C)	T_{p1} (°C)	T_{f1} (°C)	Δm_1 (%)	T_{02} (°C)	T_{p2} (°C)	T_{f2} (°C)	Δm_2 (%)	T_{03} (°C)	T_{p3} (°C)	T_{f3} (°C)	Δm_3 (%)
Starch	~ 33.5	~ 66.6	~ 130.2	~ 8.7	~ 260.1	~ 317.8	~ 393.3	~ 71.6				
Zein	~ 225.7	~ 318.9	~ 469.4	~ 68.7								
TEO	~ 32.7	~ 106.1	~ 118.8	~ 61.5	~ 120.1	~ 144.0	~ 161.5	~ 32.8				
Zein fibers	~ 35.1	~ 50.13	~ 93.74	~ 4.32	~ 222.6	~ 323.6	~ 491.4	~ 67.0				
Zein/TEO fibers	~ 34.7	~ 48.0	~ 74.5	~ 2.4	~ 78.8	~ 140.4	~ 210.6	~ 16.6	~ 227.7	~ 321.9	~ 488.0	~ 55.9
Starch film	~ 36.6	~ 60.3	~ 117.1	~ 6.6	~ 230.8	~ 325.5	~ 401.3	~ 63.8				
Bilayer film with zein fibers	~ 34.9	~ 85.0	~ 177.8	~ 11.5	~ 199.2	~ 314.0	~ 404.4	~ 69.8				
Bilayer film with zein/TEO fibers	~ 36.0	~ 72.8	~ 117.3	~ 4.2	232.0	~ 298.8	~ 396.4	~ 70.2				

TEO:Thyme essential oil. *Initial temperature (T_{0n}), peak temperature (T_{pn}), final temperature (T_{fn}), mass loss (Δm_n)

Table 4 Thickness, solubility, moisture content, water vapor permeability, tensile strength, elongation at break, adhesiveness, color parameters (L^*, a^*, b^*, and ΔE), and opacity of films

Properties	Parameters	Starch film	Bilayer film with zein fibers	Bilayer film with zein/TEO fibers
Color parameters	L^*	97.28 ± 0.48^{a}	89.70 ± 1.99^{c}	93.05 ± 1.34^{b}
	a^*	0.10 ± 0.58^{a}	-3.09 ± 0.28^{b}	-2.79 ± 0.39^{b}
	b^*	0.92 ± 0.24^{b}	8.69 ± 1.39^{a}	9.34 ± 0.55^{a}
	ΔE	1.63 ± 0.72^{c}	12.49 ± 1.65^{a}	10.80 ± 0.53^{b}
	Opacity (%)	8.6 ± 0.6^{c}	81.6 ± 7.4^{b}	95.94 ± 3.61^{a}
Physical	Thickness (mm)	0.122 ± 0.003^{c}	0.170 ± 0.006^{b}	0.194 ± 0.011^{a}
	Solubility (%)	36.5 ± 3.5^{a}	36.9 ± 0.5^{a}	35.4 ± 1.4^{a}
	Moisture content (%)	19.9 ± 2.2^{a}	19.5 ± 2.0^{a}	17.9 ± 1.1^{a}
Barrier	WVP** (g.mm/m ^{2}.day.kPa)	5.35 ± 0.18^{a}	5.50 ± 0.43^{a}	4.23 ± 0.27^{b}
Mechanical properties	Tensile strength (MPa)	7.37 ± 1.2^{a}	4.21 ± 0.8^{b}	3.74 ± 0.4^{b}
	Elongation (%)	72.8 ± 7.0^{a}	66.6 ± 6.3^{a}	72.4 ± 9.1^{a}
	Adhesiveness (g)	3.96 ± 0.86^{a}	2.91 ± 0.58^{b}	2.88 ± 0.48^{b}

The results are expressed as the mean ± standard deviation. [a,b]Different letters in the same line differ statistically ($p < 0.05$). *TEO* Thyme essential oil. ***WVP* water vapor permeability

light, reducing transparency and further intensifying opacity (Hou et al., 2024).

Opacity is an important property because it defines the amount of light that penetrates a substance, such as packaging films. An increase in opacity can be desirable in applications where light blocking is important, such as packaging that protects light-sensitive food products, preventing the degradation of nutrients and bioactive compounds (Tripathi et al., 2022). In this context, bilayer films stand out by exhibiting higher opacity compared to single-layer starch films, which showed low opacity. This characteristic gives bilayer films an additional advantage in protecting against light exposure, contributing to the greater stability of the packaged food.

Physical, Mechanical, and Barrier Properties

The results for thickness, solubility, moisture content, water vapor permeability, and mechanical properties (tensile strength, elongation, and adhesiveness) of the starch films and bilayer films are presented in Table 4. The analyzed starch films showed an average thickness ranging from 0.122 to 0.194 mm. As the compounds were added to the film structure, the thickness increased significantly. In this case, the starch film incorporated with TEO encapsulated in electrospun fibers was the thickest. During the electrospinning process of the bilayer films containing essential oil, a higher fiber yield was observed, which may explain this result. Thickness is a parameter that influences other properties of the film and should be controlled to ensure a uniform material. Factors such as composition, the amount of film-forming solution, its distribution on the mold, and the production process can affect the thickness of the films (Singh et al., 2023).

Water solubility is an important characteristic of biodegradable films, closely related to their applicability. Films with lower solubility and higher water resistance are used as packaging materials to maintain the integrity and shelf life of food products (Ballesteros-Mártinez et al., 2020). Although starch films have limitations due to their high hydrophilicity and fragility, especially for applications that require prolonged contact with moisture or water, such as in packaging for fresh or moist foods (Choi et al., 2022), in the present study, the films analyzed showed low solubility when compared to starch films from different sources (Henning et al., 2022; Oluba et al., 2021). Even after 24 h of immersion in water under agitation, no dissolution was observed. The solubility values ranged from 36.5 to 35.4%, and the moisture content ranged from 19.9 to 17.9%, with no significant difference after the incorporation of electrospun fibers ($p < 0.05$).

The water solubility of starch films can be reduced by adding hydrophobic substances to the starch matrix. Ballesteros-Mártinez et al. (2020) found similar results when using 30 to 50% glycerol as a plasticizer in sweet potato starch films, with solubility values ranging from 31.3 to 33.3%. The same authors report that higher concentrations of glycerol as a plasticizer significantly increase the water solubility of the films. This occurs due to the higher hydrophilicity of glycerol compared to other plasticizers, which reduces interactions between the polymer chains and favors plasticizer-polymer interactions. This increase disrupts the starch chain, reducing the density of hydrogen bonds and raising the water activity in the system (Ballesteros-Mártinez et al., 2020; Nogueira et al., 2018).

The water vapor permeability (WVP) of the films ranged from 5.5 to 4.23 g.mm/m^{2}.day.kPa, and the bilayer film with zein/TEO fibers showed to be a more efficient water vapor

barrier. The presence of TEO likely played a key role due to its hydrophobic nature, which contributes to reduced water transfer through the film. In addition, other factors associated with the bilayer structure, such as increased thickness, lower solubility, and reduced moisture content, may have further limited water vapor diffusion compared to the other film types. These results highlight the advantages of bilayer films in improving barrier properties and reinforce their potential for applications where moisture sensitivity is a critical concern, such as food packaging. Song et al. (2021) conducted a comparative study of starch films that exhibited high permeability in five sweet potato cultivars tested, reaching a maximum WVP of 21.43 g.mm/m^2.day.kPa.

One of the main roles of films for food packaging is to reduce moisture transfer between the food and the surrounding environment (Hosseini et al., 2013). Cai et al. (2020) produced starch films containing TEO microcapsules that decreased water vapor permeability when applied to mangoes, inhibiting weight loss and delaying ripening-related changes. Gómez-Aldapa et al. (2020) emphasize that combining two or more polymers allows the creation of new materials with improved functional properties. The authors investigated the effect of polyvinyl alcohol on the physicochemical properties of biodegradable sweet potato starch films, resulting in improved water vapor barrier properties, solubility, and mechanical performance.

Mechanical properties are essential for evaluating the structural integrity of films. In this study, the incorporation of zein electrospun fibers did not significantly alter the elongation at the break of the films. However, the tensile strength showed a reduction, ranging from 7.37 MPa in the control films (without fibers) to 3.74 MPa in the films containing fibers. Similarly, the adhesiveness of the films also decreased, varying from 3.96 to 2.88 g with the incorporation of fibers. As observed in the "Morphology" section, the deposition of zein fibers induced morphological changes in the films, possibly related to variations in temperature and humidity during the electrospinning process. These structural modifications may have altered the polymer matrix, affecting properties such as mechanical strength and adhesiveness. These results suggest that while electrospun fibers add new functionalities to the films, they may partially compromise their mechanical properties, particularly regarding strength and adhesiveness.

Despite these results, the bilayer films maintained their mechanical properties, demonstrating adequate tensile strength and elongation at break for practical applications. Estevez-Areco et al. (2020) reported improvements in cassava starch bilayer films after incorporating ZnO nanorods and PVA nanofibers loaded with rosemary extract. The values reported by the authors, with tensile strength of 3.5 MPa and elongation at a break of 76%, are comparable to those obtained in the present study.

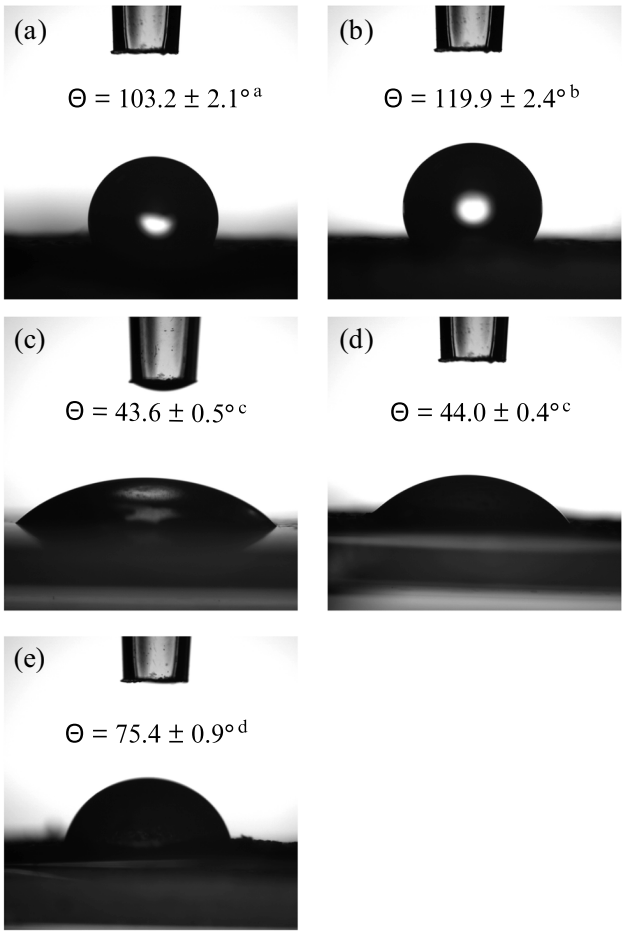

Fig. 3 Water contact angle of zein fibers (**a**), zein/TEO fibers (**b**), starch film (**c**), bilayer film with zein fibers (**d**), and bilayer film with zein/TEO fibers (**e**)

Contact Angle

The water contact angle is widely used to characterize the hydrophilicity or hydrophobicity of film surfaces. Values below 90° indicate hydrophilic surfaces, while values above 90° are characteristic of hydrophobic surfaces (Zhang et al., 2021). The water contact angle of the fibers and films is presented in Fig. 3. The value for each sample was determined by calculating the average contact angle on both sides. The zein fibers exhibited a high water contact angle of 103° and 119° for fibers with 0% and 60% of TEO, respectively. There was an increase in the contact angle with the inclusion of the EO, enhancing the hydrophobicity.

Both the starch film and bilayer films exhibited low contact angles, ranging from 43 to 75°. These results indicate that, although starch films are intrinsically hydrophilic due to the presence of hydroxyl groups, the incorporation of electrospun fibers with TEO resulted in a significant reduction in the hydrophilicity of the films (Zhang et al., 2021). This behavior can be attributed to the characteristics of the

components forming the second layer. The amino acids in zein, which constitute the fibers' matrix, possess properties that reduce the polymer's affinity for water (Nanda et al., 2024). Moreover, TEO, being a predominantly hydrophobic compound, contributes to forming a barrier that hinders the interaction between the film surface and water molecules (Mahanta et al., 2021). The incorporation of zein/TEO fibers during bilayer film production represents a promising strategy for modifying starch films, imparting more hydrophobic surface properties. This feature can expand the applications of these materials in active packaging, where moisture resistance is an essential requirement.

Biodegradability

The development of food packaging has been advancing toward recyclable, biodegradable, and compostable alternatives, aligned with the growing demands for sustainability (Han et al., 2018; Zhong et al., 2020). Biodegradation refers to the chemical decomposition of materials facilitated by the enzymatic action of microorganisms such as bacteria, yeasts, and fungi, resulting in more sustainable products (Zhong et al., 2020). In this study, sweet potato starch and zein were used for film production, natural biopolymers that enable the creation of sustainable and fully compostable packaging materials (Kola & Carvalho, 2023).

The degradation of biopolymers depends on factors such as composition, environment, type of polymer, and chemical bonds between them (Kola & Carvalho, 2023). The results of the biodegradability test for starch films and bilayer films, conducted in plant compost, are presented through photographic records, showing the progression of disintegration and curves illustrating mass loss over time (Fig. 4). After 7 days of testing, it was observed that sample deterioration began at the edges, resulting in visible irregularities. The films without fibers exhibited the highest weight loss during this initial period, and from day 21 onward, a more pronounced mass loss was evident. This trend persisted throughout the study, indicating that pure starch films underwent faster biodegradation when compared to formulations containing fibers.

At the end of the 35 days, all films demonstrated degradability potential, with significant changes in their appearance and integrity, including fragmentation, size reduction, color changes, and wrinkled surfaces. The percentage of mass loss was 45.7% for pure starch films, 28.5% for bilayer films with zein fibers, and 27.8% for bilayer films with zein/TEO fibers, indicating that the incorporation of fibers helped delay the degradation process. Polymer biodegradation is a process that can be accelerated by hydrolysis, which promotes the random breaking of polymer chains. This mechanism reduces the molecular weight of the material, making it more accessible to microbial decomposition, as reported by Asgher et al. (2020). These results highlight the influence of fibers in modulating the biodegradation rate, creating a more resistant and less susceptible matrix.

Possible explanations for the results observed may involve a combination of factors, such as the hydrophobicity of zein, which may reduce the ability of the film to absorb water—an essential factor for the hydrolysis and biodegradation of starch; the added fibers acting as a structural barrier, increasing the density and stiffness of the films and hindering the access of microorganisms and enzymes to the substrate; and the presence of TEO in the fibers, which may inhibit the growth of microorganisms responsible for degradation, further delaying the process. These factors make the bilayer films more resistant to degradation when compared to pure starch films, which have a more accessible structure and are easily degraded by microorganisms.

Although the study duration did not allow for the complete degradation of the films, the results showed a continuous mass loss over the evaluated period. This indicates that the films have the potential for biodegradation over longer timeframes. Using starch-based bilayer films with zein/TEO fibers represents a sustainable and environmentally friendly approach to managing the growing volume of solid waste, aligning with the demand for greener and more environmentally responsible solutions.

Loading Capacity and Encapsulation Efficiency of Zein Electrospun Fibers

The results of LC and EE of zein fibers are in Table 2. The LC of the fibers loaded with TEO was 33.2%, indicating that approximately one-third of the initial amount of TEO used in the production process of the fibers remained in the material. Considering that the proportion of TEO used was 60%, the LC value indicates effective incorporation of the TEO during the electrospinning process. However, previous studies show that increasing the essential oil concentration in the fibers leads to a reduction in loading capacity, likely due to saturation effects (Pires et al., 2023).

The EE was determined to be 91%, further confirming the effectiveness of the method in retaining TEO within the fibers. This result surpasses that of Ansarifar and Moradinezhad (2022), who reported an EE of 75.2% for TEO encapsulated in zein electrospun fibers. Notably, their polymer solution was prepared using glacial acetic acid as the solvent, and the TEO concentration employed was lower (4%), which differs from the methodology applied in this study. Similarly, a recent study by Valizadeh et al. (2024) achieved EE values of 92.2–96.1% and LC ranging from 12.3 to 36.1% when encapsulating pomegranate flower extract. Variations in EE can be attributed to differences in

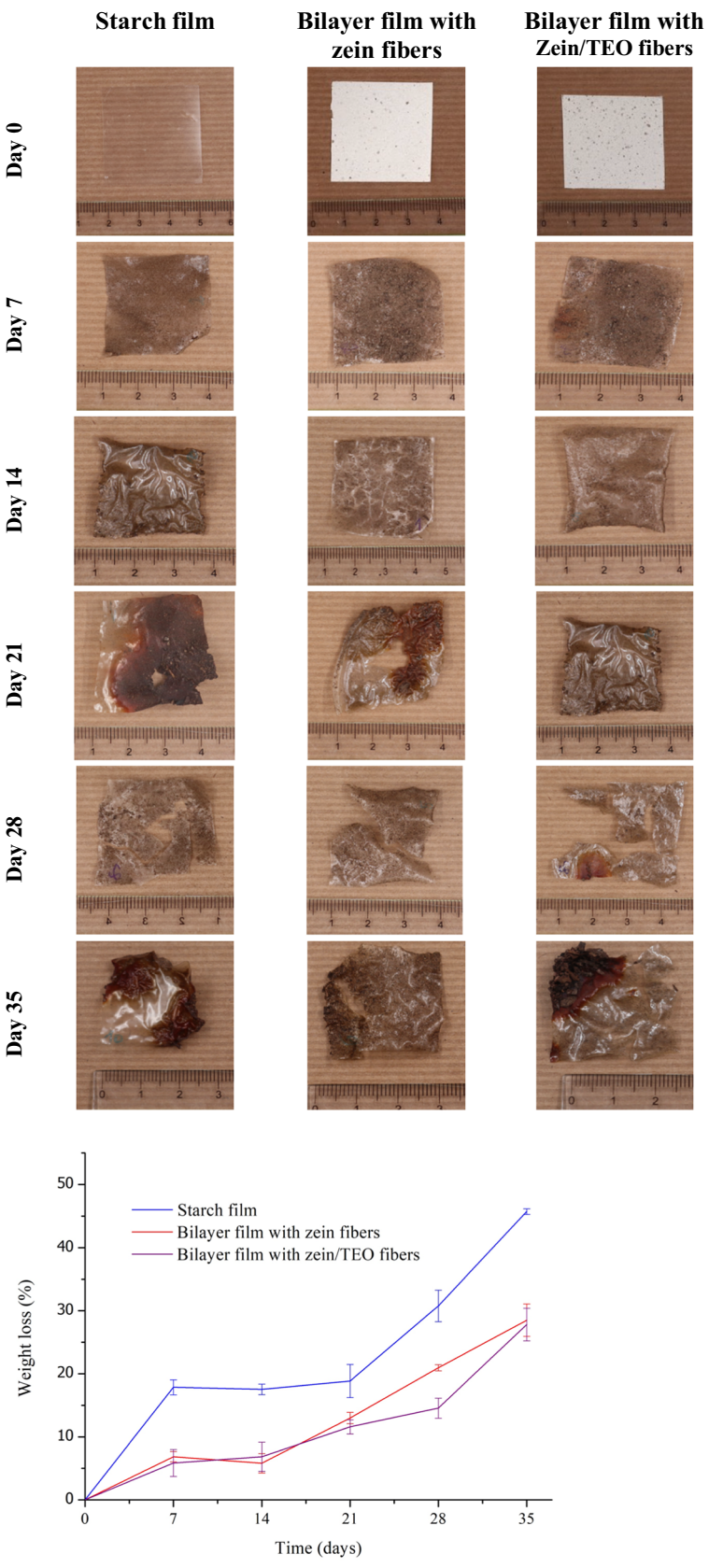

Fig. 4 Images and weight loss from the biodegradability tests of starch film, bilayer film with zein fibers, and bilayer films with zein/TEO fibers at days 0, 7, 14, 21, 28, and 35 after burial in plant compost

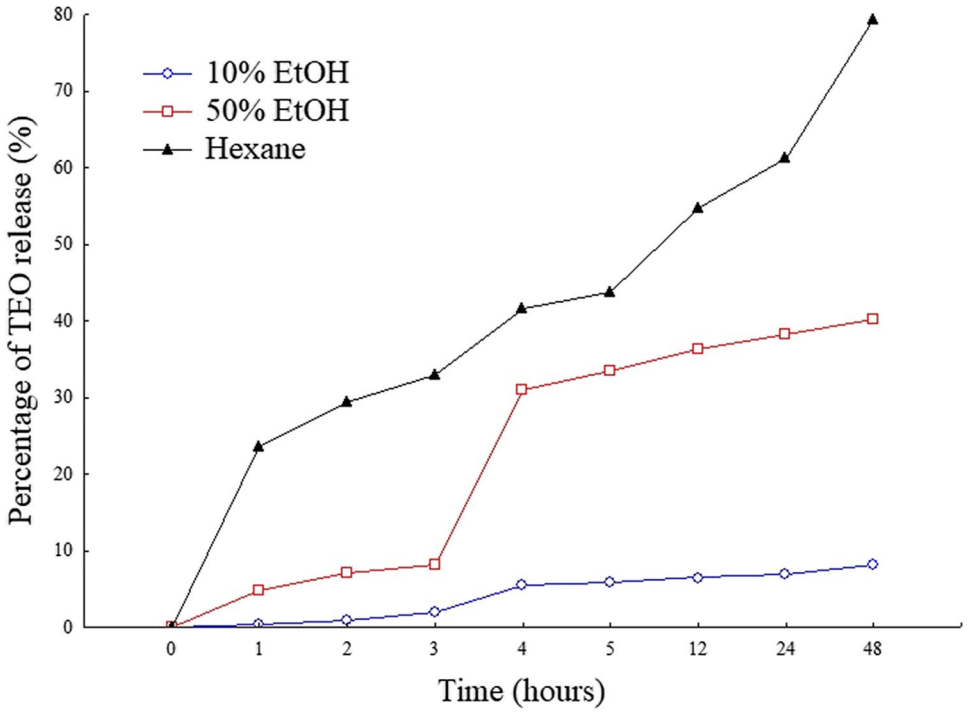

Fig. 5 In vitro release of TEO encapsulated in zein electrospun fibers in 10% ethanol (hydrophilic), 50% ethanol (lipophilic), and hexane (highly hydrophobic) media

electrospinning parameters, including applied voltage, flow rate, and needle-to-collector distance, as well as the ratio of polymer to TEO used in the formulations. The higher EE observed in this study suggests that the optimized parameters employed here enhance the encapsulation performance of the fibers, potentially offering superior protection and a more controlled release of TEO.

In Vitro Release of Essential Oil from Zein Electrospun Fibers

In vitro, release assays were performed for zein electrospun fibers incorporated with TEO using 10% ethanol (hydrophilic), 50% ethanol (lipophilic), and hexane (highly hydrophobic), by total immersion of the bilayer material in the simulants. These assays aimed to identify suitable media for the controlled release of TEO and target products for such release.

In all evaluated media, a rapid initial release of the essential oil was observed within the first 4 h, followed by a controlled release phase. After 4 h, in media containing ethanol (10% and 50%), the release exhibited a smoother slope, whereas in the more hydrophobic medium (hexane), the release profile displayed a steeper slope (Fig. 5). It was observed that the highest release of essential oil occurred in media simulating oily food models. Hexane showed the highest release, reaching 79.4% of the essential oil in the fibers after 48 h. This behavior can be attributed to the high affinity between the essential oil compounds and the hydrophobic medium, combined with the high porosity and large surface area of the electrospun fibers, which facilitate the permeation and extraction of the compounds in this medium (Fonseca et al., 2020).

Ethanol at 50% exhibited a more balanced release, reaching 40.3% of the essential oil after 48 h. On the other hand, in the hydrophilic medium (10% ethanol), the release was slower and more gradual, reaching only 8.2% after 48 h. A similar result was observed in studies with electrospun gliadin fibers loaded with essential (Bahrami et al., 2023). This behavior suggests the potential of the hydrophilic medium for applications in foods with long shelf lives, where prolonged release of bioactive compounds is desirable.

The release obtained in this assay was performed by total immersion of the bilayer material in the simulant media, representing a cumulative result from the contribution of both sides of the film. However, in real packaging applications, only one side of the film would be in contact with the food, indicating that the release of compounds in actual systems is likely to be lower than that observed in vitro.

The interaction mechanisms among the medium can explain the differences in release profiles, the encapsulating matrix (zein), and the TEO. As the polarity of the medium increases, the tendency of the hydrophobic matrix to dissolve decreases, thereby increasing the TEO release time (Bahrami et al., 2023). Furthermore, mechanisms such as diffusion and permeation through the porous structure of the fibers and their large surface area justify the initial burst release observed (Fonseca et al., 2020; Bruni et al., 2020). Additionally, encapsulation efficiency analysis

revealed that approximately 9% of the loaded TEO was not encapsulated and could be easily released during the initial hours.

In Vitro Antioxidant Activity

The antioxidant activity of TEO is directly associated with its high content of volatile compounds, as demonstrated in Table 1. Free-form TEO exhibited high antioxidant capacity, with inhibition rates of approximately 95.2% and 77.2% against ABTS and DPPH radicals, respectively. Even after the electrospinning process, fibers containing TEO displayed significant antioxidant activity for both radicals, at 76.2% and 44.3% (Fig. 6). These results can be attributed to the high concentration of encapsulated TEO (60% TEO) and the stability of the encapsulation method, which preserved the integrity of its compounds (Rather et al., 2021).

According to Bilenler et al. (2015), the antioxidant activity of TEO against radicals can occur either within the particles or after its release from the fibers. For this to happen, the encapsulated TEO must overcome the diffusion barrier imposed by the encapsulating matrix within the reaction time. In this way, antioxidants perform their function by reducing activity and neutralizing free radicals, breaking peroxides, and chelating transition metal ions. Their antioxidant efficacy is influenced by the presence of aromatic rings as well as the arrangement and quantity of hydroxyl groups (Embuscado, 2015). Dong et al. (2023), while analyzing eight distinct thyme species, identified 16 compounds positively correlated with DPPH radical scavenging capacity, with thymol, carvacrol, and p-cymene standing out.

The starch film, when evaluated in isolation, exhibited insignificant antioxidant activity for both radicals, with values below 5.6%. In contrast, zein electrospun fibers, even in the absence of TEO, demonstrated considerable antioxidant capacity, reaching 22.6% inhibition for the ABTS radical and 19.5% for the DPPH radical. These findings align with those reported by Peixoto et al. (2023) and Tavares et al. (2021) and can be attributed to the presence of specific amino acid residues in zein, such as tyrosine, tryptophan, and methionine, which possess intrinsic potential to neutralize free radicals.

The final structure of the bilayer starch film, with zein acting as the encapsulating agent for TEO, resulted in a material with antioxidant activity capable of inhibiting ABTS and DPPH radicals by 43.3% and 33.8%, respectively. These values are lower than those for free TEO; however, the TEO is protected, potentially offering prolonged and effective action. Films with antioxidant properties can play a crucial role in the preservation of food and other products by slowing the oxidation of lipids, pigments, and nutrients, as well as inhibiting the formation of toxic compounds generated by oxidative processes. This contributes to extending shelf life and enhancing the sensory quality of products (Asgher et al., 2020).

Hou et al. (2024) investigated the free radical scavenging capacity of a bilayer bioactive film made from konjac gum (KGM) and hydroxypropyl methylcellulose (HPMC), containing TEO encapsulated in a Pickering nanoemulsion. The authors observed a progressive increase in the antioxidant activity of the films with the increasing concentration of TEO, reaching maximum values of 79.9% and 89.3% inhibition against DPPH and ABTS radicals, respectively. Liu et al. (2024) developed bioactive films based on soy protein isolate incorporated with TEO and reported a significant increase in DPPH radical scavenging capacity, from 12 to 22.4%, as the concentration of TEO in the films increased.

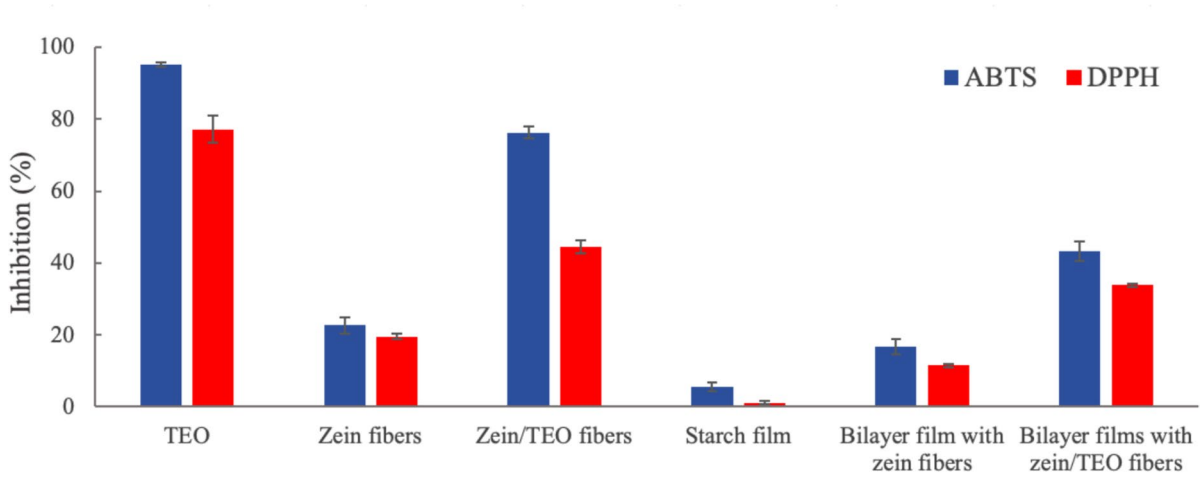

Fig. 6 Antioxidant activity of thyme essential oil (TEO), zein fibers, zein/TEO fibers, starch film, bilayer film with zein fibers, and bilayer film with zein/TEO fibers

Conclusion

Overall, the bilayer film with zein/TEO fibers demonstrated superior properties compared to monolayer starch films. These findings underscore the potential of such bilayer systems as advanced, sustainable, and functional materials for application in bioactive food packaging.

The incorporation of zein electrospun fibers containing encapsulated thyme essential oil (TEO) on the sweet potato starch–based films represented an innovative approach, resulting in an enhanced material with bioactive and biodegradable properties. The main components of TEO were identified as *p*-cymene (36.4%) and thymol (29.5%). The zein electrospun fibers with encapsulated TEO exhibited cylindrical, homogeneous, and continuous morphology without beads, classifying them as ultrafine fibers. The starch films displayed a continuous and homogeneous surface, with some cracks visible in the cross-section after fibers application, where a closely integrated bilayer structure was observed. The FTIR spectra showed characteristic bands of their components (starch, zein, and TEO), further confirming encapsulation efficiency.

The films demonstrated thermal stability, slight yellowish opacity, a thickness of 0.194 mm, low solubility, and improved water vapor barrier properties. Mechanical tests yielded satisfactory results, with an elongation at break of 72.4%, tensile strength of 3.74 MPa, and adhesiveness of 2.88 g. The films exhibited hydrophilic behavior, as indicated by the water contact angle and biodegradability, with a 27.8% mass loss over 35 days. The fibers exhibited a loading capacity of 33.2% and an encapsulation efficiency of 91%, demonstrating high effectiveness in encapsulating TEO, providing protection and controlled release, which varied depending on the medium. In vitro, the films showed antioxidant activity against DPPH and ABTS radicals. These findings underscore the potential of bilayer films as functional and sustainable packaging solutions, addressing the demand for environmentally responsible innovations in the packaging sector. The ability to incorporate bioactive compounds like TEO while maintaining the integrity of the films and performance opens new possibilities for active food packaging. However, further in situ studies are necessary to assess the long-term performance and application of the films in food preservation with controlled release of volatile compounds, particularly for sensitive products, by delaying the oxidation of lipids, pigments, and nutrients, as well as by inhibiting the formation of toxic compounds generated through oxidative processes. This approach may help protect light-sensitive foods by preventing the degradation of nutrients and bioactive compounds.

Thus, the functional differentiation between the layers allows one side to act as a mechanical barrier, while the other interacts with the food or the environment, providing bioactive protection. However, key limitations include moisture sensitivity, a common characteristic of starch-based materials, potential undesired migration of volatile compounds in more humid environments, and the need for validation through in situ studies to evaluate long-term performance and applicability in food preservation. This is especially important as the material's properties may vary depending on the type of food, secondary packaging, and storage atmosphere used. Additionally, production scale and the cost of bioactive materials remain challenges for large-scale industrial feasibility.

Supplementary Information The online version contains supplementary material available at https://doi.org/10.1007/s11947-025-03959-7.

Acknowledgements The authors gratefully acknowledge the financial support from the Coordenação de Aperfeiçoamento de Pessoal de Nível Superior (CAPES, Finance Code 001), the Conselho Nacional de Desenvolvimento Científico e Tecnológico (CNPq), and the Fundação de Amparo à Pesquisa do Estado do Rio Grande do Sul (FAPERGS, Brazil). The authors also thank CEMESUL at FURG for providing support and infrastructure for this research.

Author Contribution J.V., L.F., E.Z., and E.G. contributed to conceptualization. J.V., L.F., and T.S. performed formal analysis. J.V., L.F., T.S., and E.G. carried out the Investigation. J.V., L.F., T.S., D.C., and M.F.P. developed the Methodology. J.V. and L.F. were responsible for Data Curation. M.P., M.F.P., E.Z., and E.G. provided Resources and participated in Validation. L.F., D.C., M.F.P., M.P., E.Z., and E.G. supervised the work. J.V., L.F., T.S., and E.G. wrote the original draft. J.V., L.F., E.Z., and E.G. performed the Writing – Review & Editing. E.G., E.Z., M.F.P., and M.P. secured Funding Acquisition. E.G. managed Project Administration. All authors reviewed and approved the final manuscript.

Funding This study was funded by the Coordenação de Aperfeiçoamento de Pessoal de Nível Superior (CAPES, Finance Code 001), the Conselho Nacional de Desenvolvimento Científico e Tecnológico (CNPq), and the Fundação de Amparo à Pesquisa do Estado do Rio Grande do Sul (FAPERGS, Brazil).

Data Availability All relevant data supporting the findings of this study are included in the manuscript and its Supplementary Information. Additional data can be provided by the corresponding author upon reasonable request.

Declarations

Competing Interest The authors declare no competing interests.

References

A. D-882–91, "American Society for Testing and Materials (ASTM), tensile properties of thin plastic sheeting, standards. Annual Book of ASTM, Philadelphia," 2010. (n.d.). www.astm.org

Ansarifar, E., & Moradinezhad, F. (2022). Encapsulation of thyme essential oil using electrospun zein fiber for strawberry preservation. *Chemical and Biological Technologies in Agriculture*, *9*(1). https://doi.org/10.1186/s40538-021-00267-y

Ardjoum, N., Chibani, N., Shankar, S., Fadhel, Y. B., Djidjelli, H., & Lacroix, M. (2021). Development of antimicrobial films based on poly(lactic acid) incorporated with Thymus vulgaris essential oil and ethanolic extract of Mediterranean propolis. *International Journal of Biological Macromolecules, 185*, 535–542. https://doi.org/10.1016/j.ijbiomac.2021.06.194

Asgher, M., Qamar, S. A., Bilal, M., & Iqbal, H. M. N. (2020). Bio-based active food packaging materials: Sustainable alternative to conventional petrochemical-based packaging materials. In *Food Research International* (Vol. 137). Elsevier Ltd. https://doi.org/10.1016/j.foodres.2020.109625

Avila, L. B., Schnorr, C., Silva, L. F. O., Morais, M. M., Moraes, C. C., da Rosa, G. S., Dotto, G. L., Lima, É. C., & Naushad, M. (2023). Trends in bioactive multilayer films: Perspectives in the use of polysaccharides, proteins, and carbohydrates with natural additives for application in food packaging. In *Foods* (Vol. 12, Issue 8). MDPI. https://doi.org/10.3390/foods12081692

Azizi, H., Koocheki, A., & Ghorani, B. (2023). Structural elucidation of gluten/zein nanofibers prepared by electrospinning process: Focus on the effect of zein on properties of nanofibers. *Polymer Testing*, *128*. https://doi.org/10.1016/j.polymertesting.2023.108231

Bahrami, Z., Pedram-Nia, A., Saeidi-Asl, M., Armin, M., & Heydari-Majd, M. (2023). Bioactive gliadin electrospinning loaded with Zataria multiflora Boiss essential oil: Improves antimicrobial activity and release modeling behavior. *Food Science and Nutrition, 11*(1), 307–319. https://doi.org/10.1002/fsn3.3062

Ballesteros-Mártinez, L., Pérez-Cervera, C., & Andrade-Pizarro, R. (2020). Effect of glycerol and sorbitol concentrations on mechanical, optical, and barrier properties of sweet potato starch film. *NFS Journal, 20*, 1–9. https://doi.org/10.1016/j.nfs.2020.06.002

Basiak, E., Lenart, A., & Debeaufort, F. (2017). Effect of starch type on the physico-chemical properties of edible films. *International Journal of Biological Macromolecules, 98*, 348–356. https://doi.org/10.1016/j.ijbiomac.2017.01.122

Bhardwaj, N., & Kundu, S. C. (2010). Electrospinning: A fascinating fiber fabrication technique. In *Biotechnology Advances* (Vol. 28, Issue 3, pp. 325–347). https://doi.org/10.1016/j.biotechadv.2010.01.004

Bilenler, T., Gokbulut, I., Sislioglu, K., & Karabulut, I. (2015). Antioxidant and antimicrobial properties of thyme essential oil encapsulated in zein particles. *Flavour and Fragrance Journal, 30*(5), 392–398. https://doi.org/10.1002/ffj.3254

Böhmer-Maas, B. W., Fonseca, L. M., Otero, D. M., da Rosa Zavareze, E., & Zambiazi, R. C. (2020). Photocatalytic zein-TiO2 nanofibers as ethylene absorbers for storage of cherry tomatoes. *Food Packaging and Shelf Life, 24*, Article 100508. https://doi.org/10.1016/J.FPSL.2020.100508

Brand-Williams, W., Cuvelier, M. E., & Berset, C. (1995). *Use of a Free Radical Method to Evaluate Antioxidant Activity* (Vol. 28).

Bruni, G. P., Acunha, T. S., de Oliveira, J. P., Fonseca, L. M., Silva, F. T., Guimarães, V. M., & Zavareze, E. R. (2020). Electrospun protein fibers loaded with yerba mate extract for bioactive release in food packaging. *Journal of the Science of Food and Agriculture, 100*(8), 3341–3350. https://doi.org/10.1002/jsfa.10366

Bumedi, F., Aran, M., Miri, M. A., & Seyedabadi, E. (2023). Preparation and characterization of zein electrospun fibers loaded with savory essential oil for fruit preservation. *Industrial Crops and Products*, *203*. https://doi.org/10.1016/j.indcrop.2023.117121

Cai, C., Ma, R., Duan, M., Deng, Y., Liu, T., & Lu, D. (2020). Effect of starch film containing thyme essential oil microcapsules on physicochemical activity of mango. *LWT*, *131*. https://doi.org/10.1016/j.lwt.2020.109700

Chen, X., Cui, F., Zi, H., Zhou, Y., Liu, H., & Xiao, J. (2019). Development and characterization of a hydroxypropyl starch/zein bilayer edible film. *International Journal of Biological Macromolecules, 141*, 1175–1182. https://doi.org/10.1016/j.ijbiomac.2019.08.240

Cheng, H., Chen, L., McClements, D. J., Yang, T., Zhang, Z., Ren, F., Miao, M., Tian, Y., & Jin, Z. (2021). Starch-based biodegradable packaging materials: A review of their preparation, characterization and diverse applications in the food industry. In *Trends in Food Science and Technology* (Vol. 114, pp. 70–82). Elsevier Ltd. https://doi.org/10.1016/j.tifs.2021.05.017

Choi, I., Shin, D., Lyu, J. S., Lee, J. S., Song, H. geon, Chung, M. N., & Han, J. (2022). Physicochemical properties and solubility of sweet potato starch-based edible films. *Food Packaging and Shelf Life*, *33*. https://doi.org/10.1016/j.fpsl.2022.100867

Cruz, E. P. da, Jansen, E. T., Fonseca, L. M., Hackbart, H. C. dos S., Siebeneichler, T. J., Pires, J. B., Gandra, E. A., Rombaldi, C. V., Zavareze, E. da R., & Dias, A. R. G. (2023). Red onion skin extract rich in flavonoids encapsulated in ultrafine fibers of sweet potato starch by electrospinning. *Food Chemistry*, *406*. https://doi.org/10.1016/j.foodchem.2022.134954

D-6400−23 ASTM, "Standard specification for labeling of plastics designed to be aerobically composted in municipal or industrial facilities," 2023. (2023). ASTM International. https://doi.org/10.1520/D6400-23

Dias Antunes, M., da Silva Dannenberg, G., Fiorentini, Â. M., Pinto, V. Z., Lim, L. T., da Rosa Zavareze, E., & Dias, A. R. G. (2017). Antimicrobial electrospun ultrafine fibers from zein containing eucalyptus essential oil/cyclodextrin inclusion complex. *International Journal of Biological Macromolecules, 104*, 874–882. https://doi.org/10.1016/j.ijbiomac.2017.06.095

do Evangelho, J. A., da Silva Dannenberg, G., Biduski, B., el Halal, S. L. M., Kringel, D. H., Gularte, M. A., Fiorentini, A. M., & da Rosa Zavareze, E. (2019). Antibacterial activity, optical, mechanical, and barrier properties of corn starch films containing orange essential oil. *Carbohydrate Polymers*, *222*. https://doi.org/10.1016/j.carbpol.2019.114981

Dong, Y., Wei, Z., Yang, R., Zhang, Y., Sun, M., Bai, H., Mo, M., Yao, C., Li, H., & Shi, L. (2023). Chemical compositions of essential oil extracted from eight thyme species and potential biological functions. *Plants*, *12*(24). https://doi.org/10.3390/plants12244164

Embuscado, M. E. (2015). Spices and herbs: Natural sources of antioxidants - A mini review. In *Journal of Functional Foods* (Vol. 18, pp. 811–819). Elsevier Ltd. https://doi.org/10.1016/j.jff.2015.03.005

Estevez-Areco, S., Guz, L., Candal, R., & Goyanes, S. (2020). Active bilayer films based on cassava starch incorporating ZnO nanorods and PVA electrospun mats containing rosemary extract. *Food Hydrocolloids*, *108*. https://doi.org/10.1016/j.foodhyd.2020.106054

Fonseca, L. M., Henkes, A. K., Bruni, G. P., Viana, L. A. N., de Moura, C. M., Flores, W. H., & Galio, A. F. (2018). Fabrication and characterization of native and oxidized potato starch biodegradable films. *Food Biophysics, 13*(2), 163–174. https://doi.org/10.1007/s11483-018-9522-y

Fonseca, L. M., Radünz, M., dos Santos Hackbart, H. C., da Silva, F. T., Camargo, T. M., Bruni, G. P., Monks, J. L. F., da Rosa Zavareze, E., & Dias, A. R. G. (2020). Electrospun potato starch nanofibers for thyme essential oil encapsulation: Antioxidant activity and thermal resistance. *Journal of the Science of Food and Agriculture, 100*(11), 4263–4271. https://doi.org/10.1002/jsfa.10468

Frangopoulos, T., Marinopoulou, A., Goulas, A., Likotrafiti, E., Rhoades, J., Petridis, D., Kannidou, E., Stamelos, A., Theodoridou, M., Arampatzidou, A., Tosounidou, A., Tsekmes, L., Tsichlakis, K., Gkikas, G., Tourasanidis, E., & Karageorgiou, V. (2023). Optimizing the functional properties of starch-based biodegradable films. *Foods*, *12*(14). https://doi.org/10.3390/foods12142812

Galovičová, L., Borotová, P., Valková, V., Vukovic, N. L., Vukic, M., Štefániková, J., Ďuranová, H., Kowalczewski, P. Ł., Čmiková, N., & Kačániová, M. (2021). Thymus vulgaris essential oil and its biological activity. *Plants*, *10*(9). https://doi.org/10.3390/plants10091959

Garavand, F., Khodaei, D., Mahmud, N., Islam, J., Khan, I., Jafarzadeh, S., Tahergorabi, R., & Cacciotti, I. (2024). Recent progress in using zein nanoparticles-loaded nanocomposites for food packaging applications. In *Critical Reviews in Food Science and Nutrition* (Vol. 64, Issue 12, pp. 3639–3659). Taylor and Francis Ltd. https://doi.org/10.1080/10408398.2022.2133080

Ghasemi, M., Miri, M. A., Najafi, M. A., Tavakoli, M., & Hadadi, T. (2022). Encapsulation of Cumin essential oil in zein electrospun fibers: Characterization and antibacterial effect. *Journal of Food Measurement and Characterization, 16*(2), 1613–1624. https://doi.org/10.1007/s11694-021-01268-z

Gómez-Aldapa, C. A., Velazquez, G., Gutierrez, M. C., Rangel-Vargas, E., Castro-Rosas, J., & Aguirre-Loredo, R. Y. (2020). Effect of polyvinyl alcohol on the physicochemical properties of biodegradable starch films. *Materials Chemistry and Physics*, *239*. https://doi.org/10.1016/j.matchemphys.2019.122027

Guimarães, M. C., Marangoni Junior, L., de Souza Teodoro, C. E., Prata, A. S., & de Melo, N. R. (2024). Effect of microencapsulated thyme (Thymus vulgaris) essential oil on the antimicrobial and physicochemical properties of starch food packaging. *International Journal of Food Science and Technology, 59*(5), 3381–3390. https://doi.org/10.1111/ijfs.17087

Guo, Y., Zhang, B., Zhao, S., Qiao, D., & Xie, F. (2021). Plasticized starch/agar composite films: Processing, morphology, structure, mechanical properties and surface hydrophilicity. *Coatings*, *11*(3). https://doi.org/10.3390/coatings11030311

Han, J. W., Ruiz-Garcia, L., Qian, J. P., & Yang, X. T. (2018). Food packaging: A comprehensive review and future trends. In *Comprehensive Reviews in Food Science and Food Safety* (Vol. 17, Issue 4, pp. 860–877). Blackwell Publishing Inc. https://doi.org/10.1111/1541-4337.12343

Henning, F. G., Ito, V. C., Demiate, I. M., & Lacerda, L. G. (2022). Non-conventional starches for biodegradable films: A review focussing on characterisation and recent applications in food packaging. In *Carbohydrate Polymer Technologies and Applications* (Vol. 4). Elsevier Ltd. https://doi.org/10.1016/j.carpta.2021.100157

Heydari-Majd, M., Rezaeinia, H., Shadan, M. R., Ghorani, B., & Tucker, N. (2019). Enrichment of zein nanofibre assemblies for therapeutic delivery of Barije (Ferula gummosa Boiss) essential oil. *Journal of Drug Delivery Science and Technology*, *54*. https://doi.org/10.1016/j.jddst.2019.101290

Hosseini, F., Miri, M. A., Najafi, M., Soleimanifard, S., & Aran, M. (2021). Encapsulation of rosemary essential oil in zein by electrospinning technique. *Journal of Food Science, 86*(9), 4070–4086. https://doi.org/10.1111/1750-3841.15876

Hosseini, S. F., Rezaei, M., Zandi, M., & Ghavi, F. F. (2013). Preparation and functional properties of fish gelatin-chitosan blend edible films. *Food Chemistry, 136*(3–4), 1490–1495. https://doi.org/10.1016/j.foodchem.2012.09.081

Hou, Y., Sun, Y., Jia, S., Su, W., Cheng, S., Tan, M., & Wang, H. (2024). Double-layer films based on konjac gum and hydroxypropyl methyl cellulose loaded with thyme essential oil Pickering emulsion: Preparation, characterization, and application. *Food Hydrocolloids*, *157*. https://doi.org/10.1016/j.foodhyd.2024.110459

Jacob, J., Lawal, U., Thomas, S., & Valapa, R. B. (2020). Biobased polymer composite from poly(lactic acid): Processing, fabrication, and characterization for food packaging. In *Processing and Development of Polysaccharide-Based Biopolymers for Packaging Applications* (pp. 97–115). Elsevier. https://doi.org/10.1016/B978-0-12-818795-1.00004-6

Karim, M., Fathi, M., & Soleimanian-Zad, S. (2020). Nanoencapsulation of cinnamic aldehyde using zein nanofibers by novel needleless electrospinning: Production, characterization and their application to reduce nitrite in sausages. *Journal of Food Engineering*, *288*. https://doi.org/10.1016/j.jfoodeng.2020.110140

Kola, V., & Carvalho, I. S. (2023). Plant extracts as additives in biodegradable films and coatings in active food packaging. In *Food Bioscience* (Vol. 54). Elsevier Ltd. https://doi.org/10.1016/j.fbio.2023.102860

Kolarič, L., Minarovičová, L., Lauková, M., Karovičová, J., & Kohajdová, Z. (2020). Pasta noodles enriched with sweet potato starch: Impact on quality parameters and resistant starch content. *Journal of Texture Studies, 51*(3), 464–474. https://doi.org/10.1111/jtxs.12489

Lancuški, A., Aiman, A. A., Avrahami, R., Vilensky, R., Vasilyev, G., & Zussman, E. (2017). Design of starch-formate compound fibers as encapsulation platform for biotherapeutics. *Carbohydrate Polymers, 158*, 68–76. https://doi.org/10.1016/j.carbpol.2016.12.003

Liu, Q., Han, R., Yu, D., Wang, Z., Zhuansun, X., & Li, Y. (2024). Characterization of thyme essential oil composite film based on soy protein isolate and its application in the preservation of cherry tomatoes. *LWT*, *191*. https://doi.org/10.1016/j.lwt.2023.115686

Luo, Y., Wang, Q., & Zhang, Y. (2020). Biopolymer-based nanotechnology approaches to deliver bioactive compounds for food applications: A perspective on the past, present, and future. In *Journal of Agricultural and Food Chemistry* (Vol. 68, Issue 46, pp. 12993–13000). American Chemical Society. https://doi.org/10.1021/acs.jafc.0c00277

Mahanta, B. P., Bora, P. K., Kemprai, P., Borah, G., Lal, M., & Haldar, S. (2021). Thermolabile essential oils, aromas and flavours: Degradation pathways, effect of thermal processing and alteration of sensory quality. In *Food Research International* (Vol. 145). Elsevier Ltd. https://doi.org/10.1016/j.foodres.2021.110404

Mao, S., Li, F., Zhou, X., Lu, C., & Zhang, T. (2023). Characterization and sustained release study of starch-based films loaded with carvacrol: A promising UV-shielding and bioactive nanocomposite film. *LWT*, *180*. https://doi.org/10.1016/j.lwt.2023.114719

Martins Fonseca, L., Paulo de Oliveira, J., Lopes Crizel, R., Tavares da Silva, F., da Rosa Zavareze, E., & Dellinghausen Borges, C. (2020). Electrospun starch fibers loaded with Pinhão (Araucaria angustifolia) coat extract rich in phenolic compounds. *Food Biophysics, 15*, 355–367. https://doi.org/10.1007/s11483-020-09629-9/Published

Moradi, A., Davati, N., & Emamifar, A. (2023). Effects of Cuminum cyminum L. essential oil and its nanoemulsion on oxidative stability and microbial growth in mayonnaise during storage. *Food Science and Nutrition*, *11*(8), 4781–4793. https://doi.org/10.1002/fsn3.3457

Nanda, A., Pandey, P., Rajinikanth, P. S., & Singh, N. (2024). Revolution of nanotechnology in food packaging: Harnessing electrospun zein nanofibers for improved preservation - A review. In *International Journal of Biological Macromolecules* (Vol. 260). Elsevier B.V. https://doi.org/10.1016/j.ijbiomac.2024.129416

Nilsuwan, K., Guerrero, P., de la Caba, K., Benjakul, S., & Prodpran, T. (2020). Properties and application of bilayer films based on poly (lactic acid) and fish gelatin containing epigallocatechin gallate fabricated by thermo-compression molding. *Food Hydrocolloids*, *105*. https://doi.org/10.1016/j.foodhyd.2020.105792

Nogueira, G. F., Fakhouri, F. M., & de Oliveira, R. A. (2018). Extraction and characterization of arrowroot (Maranta arundinaceae L.) starch and its application in edible films. *Carbohydrate Polymers, 186*, 64–72. https://doi.org/10.1016/j.carbpol.2018.01.024

Nordin, N., Othman, S. H., Rashid, S. A., & Basha, R. K. (2020). Effects of glycerol and thymol on physical, mechanical, and

thermal properties of corn starch films. *Food Hydrocolloids*, *106*. https://doi.org/10.1016/j.foodhyd.2020.105884

Oluba, O. M., Osayame, E., & Shoyombo, A. O. (2021). Production and characterization of keratin-starch bio-composite film from chicken feather waste and turmeric starch. *Biocatalysis and Agricultural Biotechnology*, *33*. https://doi.org/10.1016/j.bcab.2021.101996

Ordoñez, R., Atarés, L., & Chiralt, A. (2022). Antibacterial properties of cinnamic and ferulic acids incorporated to starch and PLA monolayer and multilayer films. *Food Control*, *136*. https://doi.org/10.1016/j.foodcont.2022.108878

Otero-Herrera, A., Fuentes-Gaviria, L., Pérez-Cervera, C., & Andrade-Pizarro, R. (2025). Development of edible films based on sweet potato (Ipomoea batatas) starch and their application in candy packaging. *International Journal of Biological Macromolecules*, *299*. https://doi.org/10.1016/j.ijbiomac.2025.140031

Peixoto, E. C., Fonseca, L. M., Zavareze, E. da R., & Gandra, E. A. (2023). Antimicrobial active packaging for meat using thyme essential oil (Thymus vulgaris) encapsulated on zein ultrafine fibers membranes. *Biocatalysis and Agricultural Biotechnology*, *51*. https://doi.org/10.1016/j.bcab.2023.102778

Pires, J. B., Santos, F. N. dos, Cruz, E. P. da, Fonseca, L. M., Siebeneichler, T. J., Lemos, G. S., Gandra, E. A., Zavareze, E. da R., & Dias, A. R. G. (2024). Starch extraction from avocado by-product and its use for encapsulation of ginger essential oil by electrospinning. *International Journal of Biological Macromolecules*, *254*. https://doi.org/10.1016/j.ijbiomac.2023.127617

Pires, J. B., Santos, F. N. dos, Costa, I. H. de L., Kringel, D. H., Zavareze, E. da R., & Dias, A. R. G. (2023). Essential oil encapsulation by electrospinning and electrospraying using food proteins: A review. *Food Research International*, *170*, 112970. https://doi.org/10.1016/J.FOODRES.2023.112970

Radünz, M., dos Santos Hackbart, H. C., Camargo, T. M., Nunes, C. F. P., de Barros, F. A. P., Dal Magro, J., Filho, P. J. S., Gandra, E. A., Radünz, A. L., & da Rosa Zavareze, E. (2020). Antimicrobial potential of spray drying encapsulated thyme (Thymus vulgaris) essential oil on the conservation of hamburger-like meat products. *International Journal of Food Microbiology*, *330*. https://doi.org/10.1016/j.ijfoodmicro.2020.108696

Rather, A. H., Wani, T. U., Khan, R. S., Pant, B., Park, M., & Sheikh, F. A. (2021). Prospects of polymeric nanofibers loaded with essential oils for biomedical and food-packaging applications. In *International Journal of Molecular Sciences* (Vol. 22, Issue 8). MDPI AG. https://doi.org/10.3390/ijms22084017

Re, R., Pellegrini, N., Proteggente, A., Pannala, A., Yang, M., & Rice-Evans, C. (1999). Antioxidant activity applying an improved ABTS radical cation decolorization assay. *Free Radical Biology and Medicine, 26*(9–10), 1231–1237. https://doi.org/10.1016/S0891-5849(98)00315-3

Reddy, C. K., Choi, S. M., Lee, D. J., & Lim, S. T. (2018). Complex formation between starch and stearic acid: Effect of enzymatic debranching for starch. *Food Chemistry, 244*, 136–142. https://doi.org/10.1016/j.foodchem.2017.10.040

Reis, D. R., Ambrosi, A., & Luccio, M. Di. (2022). Encapsulated essential oils: A perspective in food preservation. In *Future Foods* (Vol. 5). Elsevier B.V. https://doi.org/10.1016/j.fufo.2022.100126

Rezaei, A., Fathi, M., & Jafari, S. M. (2019). Nanoencapsulation of hydrophobic and low-soluble food bioactive compounds within different nanocarriers. In *Food Hydrocolloids* (Vol. 88, pp. 146–162). Elsevier B.V. https://doi.org/10.1016/j.foodhyd.2018.10.003

Satyal, P., Murray, B. L., McFeeters, R. L., & Setzer, W. N. (2016). Essential oil characterization of thymus vulgaris from various geographical locations. *Foods, 5*(4), 1–12. https://doi.org/10.3390/foods5040070

Sedaghat Doost, A., Nikbakht Nasrabadi, M., Kassozi, V., Nakisozi, H., & Van der Meeren, P. (2020). Recent advances in food colloidal delivery systems for essential oils and their main components. *Trends in Food Science & Technology, 99*, 474–486. https://doi.org/10.1016/J.TIFS.2020.03.037

Silva, F. T. da, Cunha, K. F. da, Fonseca, L. M., Antunes, M. D., Halal, S. L. M. El, Fiorentini, Â. M., Zavareze, E. da R., & Dias, A. R. G. (2018). Action of ginger essential oil (Zingiber officinale) encapsulated in proteins ultrafine fibers on the antimicrobial control in situ. *International Journal of Biological Macromolecules*, *118*, 107–115. https://doi.org/10.1016/j.ijbiomac.2018.06.079

Singh, P., Kaur, G., Singh, A., Sharma, T., & Dar, B. N. (2023). Improved mechanical, functional and antimicrobial properties of corn starch-based biodegradable nanocomposites films reinforced with lemongrass oil nanoemulsion and starch nano-crystal. *Materials Chemistry and Physics*, *308*. https://doi.org/10.1016/j.matchemphys.2023.128267

Society for Testing, A. (n.d.). *E.-95 ASTM, "Standard test methods for water vapor transmission of materials. American Society for Testing and Materials," 1995.*

Sogut, E., & Seydim, A. C. (2019). The effects of chitosan- and polycaprolactone-based bilayer films incorporated with grape seed extract and nanocellulose on the quality of chicken breast fillets. *LWT, 101*, 799–805. https://doi.org/10.1016/j.lwt.2018.11.097

Song, H. geon, Choi, I., Lee, J. S., Chung, M. N., Yoon, C. S., & Han, J. (2021). Comparative study on physicochemical properties of starch films prepared from five sweet potato (Ipomoea batatas) cultivars. *International Journal of Biological Macromolecules*, *189*, 758–767. https://doi.org/10.1016/j.ijbiomac.2021.08.106

Souza, V. G. L., Mello, I. P., Khalid, O., Pires, J. R. A., Rodrigues, C., Alves, M. M., Santos, C., Fernando, A. L., & Coelhoso, I. (2022). Strategies to improve the barrier and mechanical properties of pectin films for food packaging: Comparing nanocomposites with bilayers. *Coatings*, *12*(2). https://doi.org/10.3390/coatings12020108

Springer Nature remains neutral with regard to jurisdictional claims in published maps and institutional affiliations.

Sun, K. Q., Li, F. Y., Li, J. Y., Li, J. F., Zhang, C. W., Chen, S., Sun, X., & Cui, J. F. (2019). Optimisation of compatibility for improving elongation at break of chitosan/starch films. *RSC Advances, 9*(42), 24451–24459. https://doi.org/10.1039/c9ra04053f

Tavares, W. de S., Pena, G. R., Martin-Pastor, M., & Sousa, F. F. O. de. (2021). Design and characterization of ellagic acid-loaded zein nanoparticles and their effect on the antioxidant and antibacterial activities. *Journal of Molecular Liquids*, *341*. https://doi.org/10.1016/j.molliq.2021.116915

Torres, M. R., Pires, J. B., Lemos, G. S., da Silva, F. T., de Souza, E. J. D., dos Santos, F. N., Siebeneichler, T. J., Gandra, E. A., Colussi, R., & Zavareze, E. da R. (2025). Gelatin film incorporated with pink pepper essential oil: physical properties and antimicrobial activity through direct contact and micro atmosphere. *Journal of Drug Delivery Science and Technology*, *109*. https://doi.org/10.1016/j.jddst.2025.106997

Tripathi, J., Ambolikar, R., Gupta, S., & Variyar, P. S. (2022). Preparation and characterization of methylated guar gum based nanocomposite films. *Food Hydrocolloids*, *124*. https://doi.org/10.1016/j.foodhyd.2021.107312

Valizadeh, R., Zandi, M., Ganjloo, A., & Dardmeh, N. (2024). Electrospun zein fibers loaded with pomegranate flower extract: Characterization and release behavior. *Food Bioscience*, *62*. https://doi.org/10.1016/j.fbio.2024.105217

Vannini, M., Marchese, P., Sisti, L., Saccani, A., Mu, T., Sun, H., & Celli, A. (2021). Integrated efforts for the valorization of sweet potato by-products within a circular economy concept:

Biocomposites for packaging applications close the loop. *Polymers*, *13*(7). https://doi.org/10.3390/polym13071048

Wang, P., Li, Y., Zhang, C., Feng, F., & Zhang, H. (2020). Sequential electrospinning of multilayer ethylcellulose/gelatin/ethylcellulose nanofibrous film for sustained release of curcumin. *Food Chemistry*, *308*. https://doi.org/10.1016/j.foodchem.2019.125599

Wu, F., Misra, M., & Mohanty, A. K. (2021). Challenges and new opportunities on barrier performance of biodegradable polymers for sustainable packaging. In *Progress in Polymer Science* (Vol. 117). Elsevier Ltd. https://doi.org/10.1016/j.progpolymsci.2021.101395

Wu, H., Wang, J., Li, T., Lei, Y., Peng, L., Chang, J., Li, S., Yuan, X., Zhou, M., & Zhang, Z. (2023). Effects of cinnamon essential oil-loaded Pickering emulsion on the structure, properties and application of chayote tuber starch-based composite films. *International Journal of Biological Macromolecules*, *240*. https://doi.org/10.1016/j.ijbiomac.2023.124444

Zhang, C., Chen, F., Meng, W., Li, C., Cui, R., Xia, Z., & Liu, C. (2021). Polyurethane prepolymer-modified high-content starch-PBAT films. *Carbohydrate Polymers*, *253*. https://doi.org/10.1016/j.carbpol.2020.117168

Zhong, Y., Godwin, P., Jin, Y., & Xiao, H. (2020). Biodegradable polymers and green-based antimicrobial packaging materials: A mini-review. In *Advanced Industrial and Engineering Polymer Research* (Vol. 3, Issue 1, pp. 27–35). KeAi Communications Co. https://doi.org/10.1016/j.aiepr.2019.11.002

Authors and Affiliations

Jéssica Silveira Vitoria[1] · Laura Martins Fonseca[2] · Tatiane Jéssica Siebeneichler[2] · Débora Campos[3] · Fátima Poças[3] · Maria Manuela Estevez Pintado[3] · Elessandra da Rosa Zavareze[2] · Eliezer Avila Gandra[1]

✉ Jéssica Silveira Vitoria
jessicasilveiravitoria@gmail.com

Laura Martins Fonseca
laura_mfonseca@hotmail.com

Tatiane Jéssica Siebeneichler
tatijs1@hotmail.com

Débora Campos
dcampos@ucp.pt

Fátima Poças
fpocas@ucp.pt

Maria Manuela Estevez Pintado
mpintado@ucp.pt

Elessandra da Rosa Zavareze
elessandrad@yahoo.com.br

Eliezer Avila Gandra
gandraea@hotmail.com

[1] Laboratory of Microbiology and Food Science (LACIMA), Graduate Program in Nutrition and Food, Center for Chemical, Pharmaceutical, and Food Sciences, Federal University of Pelotas, Pelotas, RS 96010-900, Brazil

[2] Laboratory of Biopolymers and Nanotechnology in Food (BioNano), Department of Agro-Industrial Science and Technology, Graduate Program in Food Science and Technology, Federal University of Pelotas, Pelotas, RS 96010-900, Brazil

[3] College of Biotechnology, Portuguese Catholic University, 4169-005 Porto, Portugal